

Journal Pre-proof

Strike-slip related folding within the Malvinas/Falkland Trough (south-western Atlantic ocean)

F.D. Esteban, J.P. Ormazabal, F. Palma, L.E. Cayo, E. Lodolo, A.A. Tassone



PII: S0895-9811(19)30398-0

DOI: <https://doi.org/10.1016/j.jsames.2019.102452>

Reference: SAMES 102452

To appear in: *Journal of South American Earth Sciences*

Received Date: 4 August 2019

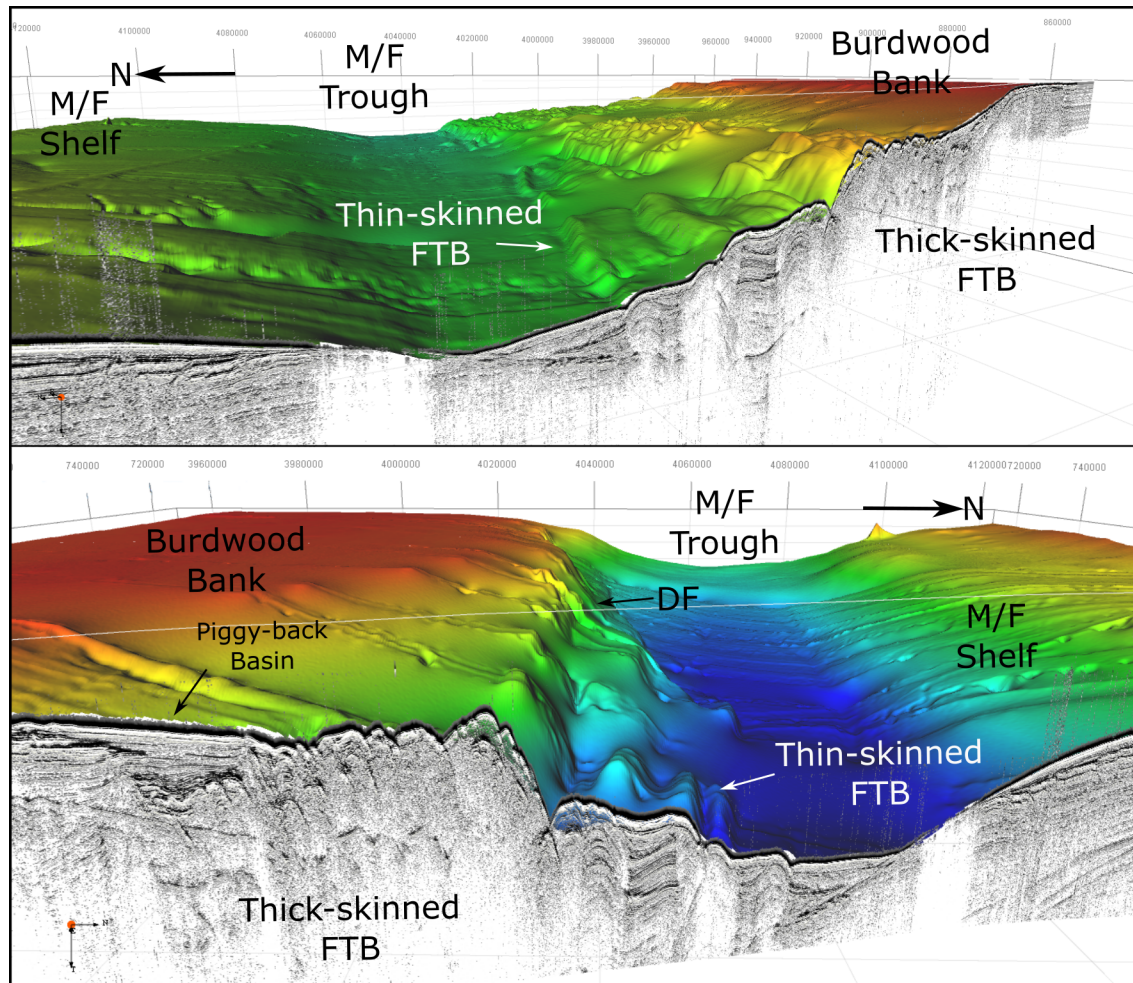
Revised Date: 2 December 2019

Accepted Date: 2 December 2019

Please cite this article as: Esteban, F.D., Ormazabal, J.P., Palma, F., Cayo, L.E., Lodolo, E., Tassone, A.A., Strike-slip related folding within the Malvinas/Falkland Trough (south-western Atlantic ocean), *Journal of South American Earth Sciences* (2020), doi: <https://doi.org/10.1016/j.jsames.2019.102452>.

This is a PDF file of an article that has undergone enhancements after acceptance, such as the addition of a cover page and metadata, and formatting for readability, but it is not yet the definitive version of record. This version will undergo additional copyediting, typesetting and review before it is published in its final form, but we are providing this version to give early visibility of the article. Please note that, during the production process, errors may be discovered which could affect the content, and all legal disclaimers that apply to the journal pertain.

© 2019 Published by Elsevier Ltd.



Strike-slip related folding within the Malvinas/Falkland Trough (south-western Atlantic Ocean)

Esteban F.D., Ormazabal J.P., Palma F., Cayo L.E., Lodolo E., Tassone A.A.

Abstract

The Malvinas/Falkland Trough (M/FT) is an E-W trending bathymetric depression along which runs the present-day South American-Scotia plate boundary. To the north of the M/FT lies the southern sector of the South Malvinas/Falkland Basin, and to the south lies the Burdwood Bank, an elongated morphological high constituting part of the South Scotia Ridge. Analysis of bathymetric and slope maps, integrated with seismic reflection profiles, have allowed describing in detail the M/FT in the sector comprised between 60° and 57° W. Data show the presence of an array of folds forming a thin-skinned fold-and-thrust Belt (FTB), previously interpreted as an active compressional field. The thin-skinned FTB is developed in a triangular-shaped area, which extends *ca.* 100 km in the E-W direction and 16 km in the N-S direction. Four parallel, asymmetric folds that develop to progressively greater water depths (between 1600-2600 m depth) towards the north, with orientations ESE-WNW and lengths that vary between 22 and 98 km, have been recognized. These folds are constituted by Late Cenozoic sediments that are undeformed in the Malvinas/Falkland Trough. The development of folds, which began in the late Miocene (*ca.* 7 Ma), was associated with the left-lateral strike-slip tectonic regime of the Magallanes-Fagnano-Malvinas lineament, the western segment of the South American-Scotia plate boundary.

Keywords:

North Scotia Ridge, Morpho-bathymetry, slope maps, geomorphometry, seismic reflection profiles, fold arrays, strike-slip tectonics.

1 Introduction

The Malvinas/Falkland Trough is a bathymetric depression that may have formed as an orogenic foredeep (Dalziel et al., 1974a; Dalziel and Palmer, 1979). It was formed by the flexure of the southern edge of the South American Plate when colliding against the Burdwood Bank (Fig. 1; Ludwig and Rabinowitz 1982; Richards et al. 1996; Bry et al. 2004). Nowadays it extends in an E-W direction between the North Scotia Ridge to the south and the Malvinas/Falkland Shelf and Malvinas/Falkland Plateau to the north. It is part of the Magallanes-Fagnano-Malvinas (MFM) left-lateral plate boundary between the South America

and Scotia plates (Fig. 1; Pelayo and Wiens, 1989; Lodolo et al., 2002, 2003; Thomas et al., 2003; Smalley et al., 2003, 2007; Torres Carbonell et al., 2014).

In its western sector, north of Burdwood Bank between 60° and 57° W, there is a series of folds that have been interpreted as evidence of active compression (Ludwig and Rabinowitz, 1982; Platt and Philip, 1995; Richards et al., 1996; Bry et al., 2004). Other authors, alternatively propose that there is a strike-slip component of deformation superimposed to these structures (Richards et al., 1996; Stone, 2016). However, strike-slip structures have not been described in this sector even though the MFM lineament has been active since the late Miocene (Lodolo et al., 2002, 2003; Tassone et al., 2008; Torres Carbonell et al., 2014). Transtensive and transpressive structures have been identified both onshore and offshore along the MFM lineaments towards the E and W (Cunningham et al., 1998; Cunningham, 1998; Lodolo et al., 2003; Del Ben and Mallardi, 2004; Esteban, 2014; Esteban et al., 2018).

In this work, from the use of slope maps integrated with seismic reflection profiles (Esteban et al., 2017) we: (i) describe the geometry and size of the folds in plain view; (ii) interpret their origin within the regional geological framework and the prevailing tectonic regime; (iii) present an evolutionary model for the region.

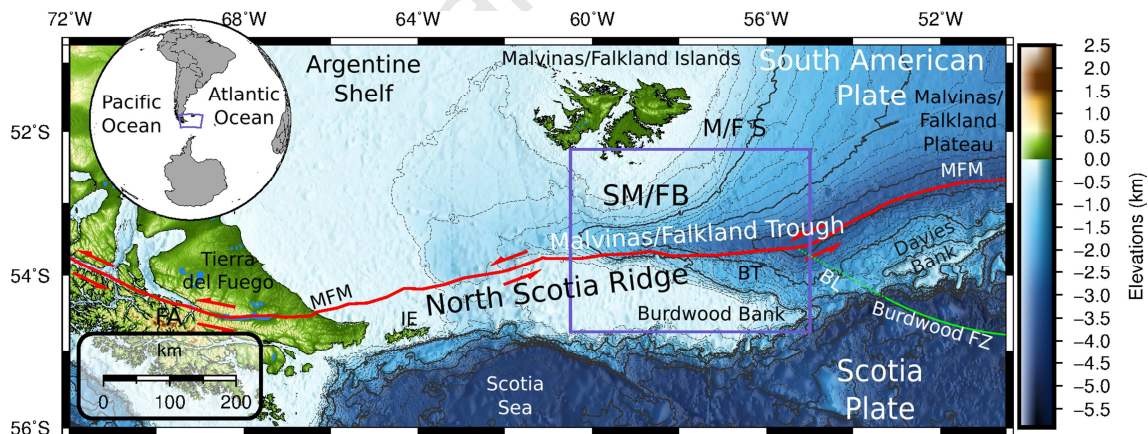


Figure 1: Bathymetric map (source SRTM15_plus) with the location of the study area (blue box). Plate boundary from Esteban et al. (2018). BL: Burdwood Lineament. BT: Burdwood Terrace. IE: Isla de Los Estados. FA: Fuegian Andes. FZ: Fracture Zone. MFM: Magallanes-Fagnano-Malvinas lineament. M/FS: Malvinas/Falkland Shelf. SM/FB: South Malvinas/Falkland Basin.

2 Geologic Framework

2.1 Regional geology

The study area is located to the north of the Burdwood Bank, in the southern sector of the South Malvinas/Falkland Basin (Fig. 1). It spans from the Burdwood Bank and Burdwood Terrace up to the Malvinas/Falkland Shelf, which is separated by the Malvinas/Falkland Trough. This tectonic depression coincides with the current South American-Scotia plate boundary which extends for more than 3,000 km from Tierra del Fuego to the Georgia Island (Forsyth, 1975; Pelayo and Wiens, 1989; Lodolo et al., 2002, 2003; Giner-Robles et al., 2003; Esteban et al., 2012, 2013; Torres Carbonell et al., 2014). The main tectonic units and regimes of this area are in Table 1.

The Burdwood Bank is part of the western segment of the North Scotia Ridge (Davey, 1972; Esteban et al., 2010). It is considered an eastward extension of the Fuegian Andes, so it is presumed that it is composed of Cenozoic metamorphic rocks like those found in southern Tierra del Fuego and Isla de Los Estados (Dalziel et al., 1974a; Dalziel and Palmer, 1979; Caminos and Nullo, 1979; Olivero and Malumián, 2008).

The Malvinas/Falkland Shelf is the sector of the Argentine Shelf that surrounds the homonymous islands (Fig. 1). Its basement is covered by Paleozoic units similar to the outcrops in the islands, over which a Meso-Cenozoic sedimentary fill has been deposited (Richards et al., 1996; Fish, 2005; Koenitz et al., 2008; Foschi and Cartwright, 2016; Stone, 2016). The South Malvinas/Falkland Basin spans from the shelf border up to the Malvinas/Falkland Trough. It has an E-W orientation and corresponds to a typical foreland basin (Platt and Philip, 1995; Bry et al., 2004; Foschi and Cartwright, 2016).

In the basin, Foschi and Cartwright (2016) identified two main units based on a regional unconformity. Available well data (61/17-1) indicates that their lower units (1A and 1B) are of Mesozoic age while the upper unit (2) is of Cenozoic age (Foschi and Cartwright, 2016; Foschi et al., 2019; Table 1). The lower unit is interpreted as sediments associated with the pre-rift, syn-rift and sag stages, which lie in the Malvinas/Falkland Shelf. The upper unit is composed of sediments and can be divided into two sub-deposits. The first is located in the SW sector of the Malvinas/Falkland Shelf which constitutes a Neogene drift deposit developed under the Antarctic Circumpolar Current activity (Bry et al., 2004; Koenitz et al., 2008; Pérez et al., 2015; Weber et al., 2019). Koenitz et al. (2008) studied the drift with multi-channel seismic profiles and identified four units (1A, 1B, 2A, 2B, Table 1). The age of the unconformities (that defined the units) was inferred from the correlations with major climatic and oceanic circulations (sedimentary) events. Pérez et al. (2015) later reassigned the age of the unconformities (and units) based on the tectonic evolution of the Scotia Sea. Preliminary

results of the recent 382 IODP expedition found that the sequences of the drift deposit are much younger (Weber et al., 2019). During the expedition, the two extracted cores (U1534 and U1535) reached the reflectors A, B and C, which correspond to the top of the sub-units 2A, 1B and 1A of Koenitz et al., (2008), respectively. The ages of the reflectors, based on preliminary bio-magnetostratigraphy, indicate that the deposits above Reflector B are Pleistocene in age (no older than 0.78 Ma; Brunhes Chron C1n), between reflectors B and C are of Late Pliocene age (2.58 - 3.6 Ma) and below Reflector C are of early Pliocene age (4.1-4.7 Ma).

The second deposit of the Cenozoic unit is located in the Malvinas/Falkland Trough and forms a wedge-shaped deposit that thickens towards the Burdwood Bank with a maximum thickness of nearly 3 km (Foschi and Cartwright, 2016) and constitutes the foreland in a strict sense (Bry et al., 2004; Fish, 2005). Koenitz et al. (2008) roughly identified four units (I-IV; Table 1). The age of these units was based on tectonic events and its stratigraphic relationship with the drift deposit units. Unit I shows stratigraphic growth, which indicates that it is coeval with the deformation and predates Unit 1A. The unit II shows less stratigraphic growth and broadly correlates with unit 1A. The units III and IV do not show stratigraphic growth, which indicates a predominant coeval strike-slip deformation and broadly correlates with unit 2B.

The core 13/14-2 in the Malvinas/Falkland Trough found a Holocene-Pleistocene (upper 84 cm, biozone NN21) to late Pliocene (lower 127 cm, biozone NN15, *ca.* 3.8 Ma) sequence based on calcareous nannofossils (Cusminsky, 1991; Rivas et al., 2018). This core presents lithological/paleontological characteristics similar to KC099 (Howe et al., 1997; Cunningham et al., 2002). Both show *ca.* 30 cm of foraminifera sands, followed by diatomaceous muds (Espósito, 1981; Howe et al., 1997). These sequences could be correlated with the units IV and maybe III of Koenitz et al. (2008), respectively (Table 1) and with the drift sediments located in the mini basins between the anticlines located in the south (Foschi et al., 2019). Within this deposit, mass transport deposits with variable thickness (100-300 m), which originated adjacent to the northern margin of the Burdwood Bank, along with four types of direct hydrocarbon indicators, were identified (Foschi and Cartwright, 2016; Foschi et al., 2019). These deposits are frequently triggered by tectonic deformation associated with earthquakes (Pérez et al. 2016; Ormazabal et al. 2019). The new ages for the drift sequences (Weber et al., 2019) would indicate that the Unit I could be up to Miocene-Pliocene? (older than 4.7 Ma), while the Unit II would be Miocene?-Pliocene and the Units III and IV are Quaternary.

In the southern sector of the Malvinas/Falkland Trough, part of the sedimentary sequences is folded (Bry et al., 2004; Koenitz et al., 2008; Foschi and Cartwright, 2016; Foschi et al., 2019) indicating that the belt comprises a series of thrust-propagation anticlines with ESE-WNW axis. Bry et al. (2004) described that the faults and folds are the manifestations of regional shortening, and they identified a thin-skinned deformation developed over underformed Mesozoic sequences (with good resolution in the seismic sections), and a thick-skinned deformation (characterized by narrow basement ridges and incoherent reflectors). Ludwig and Rabinowitz (1982) interpreted the sediments of the Malvinas/Falkland Trough as a collision complex (or accretionary prism) with active deformation. In the seismic section (the same shown here) they show folding and uplift of trough sediments onto the north side of the North Scotia Ridge while in line 144 (located 156 km towards the E on the Malvinas/Falkland Trough) the sediments are deformed. The deformation is confined in the upper sector (1 to 3 s two-way travel time; TWT) while the lower layers are not deformed. These deformed sequences correspond to the Burdwood Terrace, which is an area to the NE of the Burdwood Bank characterized by a rough surface and intermediate water depths that increase towards the NW (Fig. 1; Esteban et al., 2017).

Although a transpressive regime has been proposed for the southern part of the South Malvinas/Falkland Basin, structures related to this regime have not been described, and instead, active thrusting has been described on the northern flank of Burdwood Bank Ludwig and Rabinowitz, 1982; Platt and Philip, 1995; Richards et al., 1996; Bry et al., 2004). Ghiglione et al. (2010) indicated that the Burdwood Bank was elevated partly due to transpression. Richards et al. (1996, p.112) indicated that “most faults within the basin trend generally E-W and may have a major strike-slip component but look superficially like true normal faults”.

The seismic stratigraphy of the South Malvinas/Falkland Basin allows us to constrain the deformation age. Several authors agree on a post-Miocene deformation (Table 1). Within the sedimentary fill of the Malvinas/Falkland Trough, Koenitz et al. (2008) observed that normal faulting and stratigraphic growth affect the Paleogene units of the Malvinas/Falkland Trough (I and II, Table 1), and infer a late Miocene - Quaternary strike-slip tectonics coeval with units III and IV. Fish (2005) assigns a late Eocene-Miocene age to the deformed sedimentary sequence (Foreland Fill II) and Pliocene-Holocene to the overlying undeformed unit (Post foreland fill). This last unit was then reinterpreted by Ghiglione et al. (2010) as syn-orogenic based on two indicators (abrupt thinning and progressive unconformities). This indicates that the folding was active after 5 Ma (Table 1). However, the new ages of the drift deposit (Weber et al., 2019) would indicate that the folding is younger.

Detailed studies based on corings, side-scan sonar and seismic reflection profiles were realized in the North Scotia Ridge and the Malvinas/Falkland Trough (Cunningham and Barker, 1996; Cunningham, 1998; Cunningham et al., 1998, 2002). These studies show the tectonic and sedimentary environment to the east of the Burdwood Bank (between 58° W and 40° W). They found that the N-S convergence has ceased along the Malvinas/Falkland Trough since the accretionary prism of the North Scotia Ridge was buried beneath undeformed sediment drifts (Cunningham and Barker, 1996; Cunningham et al., 1998). Within the North Scotia Ridge accretionary prism a stripped acoustic fabric was identified between 48.5° W and 54° W (NR1; Cunningham et al., 1998). It is characterized by sub-parallel lineaments closely aligned with the bathymetric contours that are attributed to well-formed, open folds that progressively deepens to the north based on seismic reflection profiles.




		Tectonic Regime	South Malvinas/Falkland Basin								M/F Trough	Burdwood Bank	This work				
			Rivas18 13-14/2 Quat. (NN21)	Howe97 KC099 Quat.	Bry04 M/FSM/FT	Fish05	Koenitz08 M/FS M/FT	Pérez15	Foschi 2016	Weber19 U1534U1535	Del Ben 2004	Parker96	BB	M/F			
Cenozoic	Quaternary	 Strike-slip and Drifting		Contomita	Foreland Wedge	Post foreland fill	2B	IV	Unit I	Unit 2	I A	G	Piggy Back Basins				
	2.6 Ma							Horizon-a	III B								
	Pliocene							III	Unit II		C II ?						
	5.3 Ma	2A						Horizon-b	II		F3						
	Miocene	1B						Unit III									
	23 Ma	1A						Unit IV									
								Unit V									
								Basement Top									
	Oligocene	I						Foreland Fill II	Unit 2		F1					?	?
	33.9 Ma																
Eocene																	
56 Ma																	
Paleocene	Foreland Fill I																
Mesozoic	Late Cretaceous	 Collision		Mesozoic	Synrift II	Postrift II		Unit 1b	"Basement"	Unit 1a	C-D-E	Low-grade Metamorphic Rocks	B1	M1			
	100 Ma																
	Early Cretaceous														Sag		
	145 Ma	 Syn-Rift															
	Late																
Jurassic	Middle		Synrift I														
	Paleozoic	Pre-Rift	Basement	Basement				Base.									

Table 1: Chrono-stratigraphic chart with the main geologic units and the dominant tectonic regime of the SW Atlantic Ocean. Tectonic regime from Bry et al. (2004); Fish (2005); Tassone et al. (2008). BB: Burdwood Bank. M/FT: Malvinas/Falkland Trough. M/FS: Malvinas/Falkland Shelf.

171

172 **2.2 Tectonic background**

173 The tectonic evolution of the extreme south of South America is the result of different
174 tectonic regimes developed from the late Paleozoic to the present (Dalziel et al., 1974b;
175 Nelson et al., 1980; Klepeis and Austin, 1997; Barker, 2001; Tassone et al., 2008; Menichetti et
176 al., 2008; Herve et al., 2010; V  rard et al., 2012; Dalziel et al., 2013; Ghiglione, 2016). From the
177 Cambrian to the Middle Jurassic, the southern tip of South America was part of Gondwana
178 (Herv   et al., 2010). Following the Gondwana breakup between the Middle and Late Jurassic,
179 the region was affected by generalized extension, which gave rise to the Southern
180 Malvinas/Falkland Basin, among other offshore basins (Uliana et al., 1989; Galeazzi, 1998; Bry
181 et al., 2004; Tassone et al., 2008; Raggio et al., 2011; Barist  as et al., 2013; Lovecchio et al.,
182 2019). The initial rifting phase was followed by thermal subsidence during the Cretaceous (Bry
183 et al., 2004; Tassone et al., 2008; Barist  as et al., 2013).

184 During the Mesozoic the Burdwood Bank, along with other continental fragments that
185 presently compose the North Scotia Ridge, were grouped together and connected to form a
186 bridge of continental crust between the Antarctic Peninsula and South America (Barker, 2001;
187 Livermore et al., 2005; Eagles, 2010; V  rard et al., 2012; Dalziel et al., 2013; Eagles and Jokat,
188 2014; Eagles, 2016). The development of the Scotia Plate (and Sea) controlled the relative
189 movement of the Burdwood Bank with respect to the Malvinas/Falkland Shelf and the opening
190 of the Drake Passage during the Cenozoic (Barker, 2001; Dalziel et al., 2013; Eagles and Jokat,
191 2014). During the Oligocene (*ca.* 28 Ma), with the spreading of the West Scotia Ridge several
192 segments separated by fractures zones developed in the western Scotia Sea (Dalziel et al.,
193 2013; Eagles et al., 2005; Livermore et al., 2005; Lodolo et al., 2006; Eagles and Jokat, 2014;
194 Eagles, 2016). This spreading produced a migration of the Burdwood Bank and convergence
195 northward and northeast against the Malvinas/Falkland Shelf with the subsequent collision
196 (Barker, 2001; Lodolo et al., 2006; Eagles and Jokat, 2014; Torres Carbonell et al., 2014;
197 Ormazabal et al., 2019). Data analysis suggests that there are structural lineaments (such as
198 the Burdwood Lineament) that coincide with the fracture zone (Burdwood Fracture Zone) and
199 extend northwards up to the South American-Scotia Plate Boundary (Fig. 1; Esteban, 2014;
200 Esteban and Tassone, 2017).

201 In the late Miocene-Pliocene (*ca.* 6 Ma), the cessation of expansion of the Scotia Plate
202 (Lodolo et al., 2006) caused the development of the current plate boundary, the Magallanes-
203 Fagnano-Malvinas lineament which extends in the E-W direction from the Isla de Tierra del

Fuego, the northern border of the North Scotia Ridge and the Malvinas/Falkland Trough (Klepeis, 1994; Cunningham et al., 1998; Lodolo et al., 2002, 2003; Esteban et al., 2011, 2012; Betka et al., 2016). Other authors indicated an age of 7-10 Ma for the onset of the lineament (Torres Carbonell et al., 2008, 2014). The horizontal displacement along the plate boundary has been estimated in Tierra del Fuego between 20 and 55 km (Klepeis, 1994; Olivero and Martinioni, 2001; Rossello, 2005; Torres Carbonell et al., 2008). Earthquake data show that this lineament is still active (Forsyth, 1975; Pelayo and Wiens, 1989; Thomas et al., 2003; Bohoyo et al., 2019) with E-W relative movements measured with GPS between 4.4 and 6.6 mm/a (Smalley et al., 2003, 2007; Mendoza et al., 2011, 2015). Transtensional structures have been developed along the plate boundary in Tierra del Fuego and the Argentine Shelf (Lodolo et al., 2003; Malumián and Olivero, 2005; Tassone et al., 2008; Esteban et al., 2014; Onorato et al., 2016; Esteban et al., 2018).

3 Data and methods

3.1 Database

For this study, 28 seismic profiles with a total length of 4,500 km were analyzed (Fig. 2). The database, which covers an area of 15,000 km², is composed of multi-channel and single-channel seismic reflection profiles (Table 2). The multi-channel data were kindly provided by the Secretaría de Energía Argentina and were acquired during two surveys carried out between 1977 and 1978 (RC2106, see <http://www-udc.ig.utexas.edu/sdc/cruise.php?cruiseIn=rc2106> for more information; Ludwig and Rabinowitz, 1982; Ludwig, 1983). The single-channel seismic profiles were acquired between the '60 and '70 (DSDP-360, RC1505, RC1801, V3103) and were downloaded from the GeoMapApp site (<http://www.geomapapp.org>) and National Centers for Environmental Information (NCEI; <https://maps.ngdc.noaa.gov/viewers/geophysics/>). Seismic sections published by different authors were also integrated into the database (Table 2) and correspond to 2-D multi-channel seismic surveys conducted since 1993 (Platt and Philip 1995; Richards et al. 1996; Bry et al. 2004; Fish 2005; Koenitz et al. 2008; Foschi and Cartwright 2016) and 3-D seismic surveys (Foschi et al., 2019).

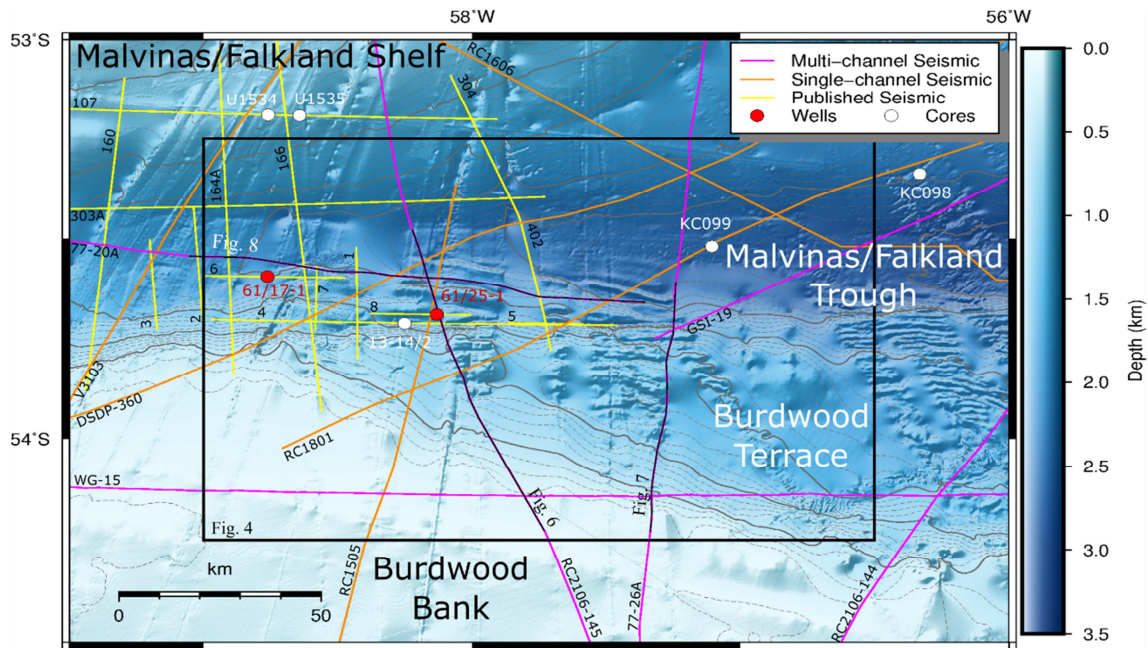


Figure 2: Detailed bathymetric map of the Malvinas/Falkland Trough area (source: DBM-

BATDRAKE) with contour lines every 100 m (dashed lines) and 500 m (solid lines). See auxiliary table for details.

The bathymetric grid DBM-BATDRAKE (Bohoyo et al. 2019) was used in this study, which has a resolution of 200 x 200 m. In the study area, the grid combines multi-beam data from transits from/to Malvinas/Falkland Islands and depths predicted by satellite data (GEBCO_2014; see Fig. 2 of Bohoyo et al., 2019). This combination of sources is seen in the bathymetric and slope maps (Figs. 2 and 3) as areas of higher- and lower-resolution, respectively. A detailed multi-beam survey (MV1204) available at GMRT (<https://www.gmrt.org/>; Ryan et al. 2009) was also used in this study; it has a resolution of 36 x 36 m. In the maps, linear artifacts associated with the integration of the different sources can be identified. We also analyzed the bathymetric map in raster format elaborated by Foschi et al. (2019), which shows a detailed map derived from 3-D seismic data. It is important to clarify that none of the seismic data was used for deriving seafloor bathymetry.

Data from the cores 13/14-2 (Espósito 1981; Cusminsky 1991; Rivas et al. 2018), KC099 (Cunningham and Barker, 1996; Howe et al., 1997; Cunningham et al., 2002) and wells (61/17-1 and 61/25-1; Foschi and Cartwright 2016; Foschi et al. 2019) were used, as well as cores (U1534 and U1535) from the recent 382 IODP expedition (Weber et al., 2019). This information allowed constraining the age of the identified seismic units.

Source	# Lines	Lines	km recorded	km recorded
SC	5	18 %	1743	38 %
MC	8	29 %	2098	46 %
PB	15	54 %	689	15 %
Total	28	100 %	4530	100 %

Table 2: Seismic reflection data used in this study. PB: Published. MCS: Multi-channel seismic profiles. SCS: Single-channel seismic profiles.

3.2 Processing and methods

The interpretation and integration of the data were made with the IHS Kingdom Software (v. 2016). For some specific seismic profiles a Pseudo-Relief Attribute (TecVA, Bulhões and de Amorim, 2005) was calculated, with the aim of highlighting the geometry and acoustic characteristics observed in the seismic profile. The seismic sections in raster format were transformed into SEG-Y standard format (Hagelund and Levin, 2017) with the Image2Segy software (Farran, 2008). The Generic Mapping Tools software was used (GMT v. 5.4; Wessel et al., 2013) to elaborate the grid slope from the bathymetric data and to produce most of the figures. The resulting grids have the same resolution as the original data (200 or 36 m). Slope maps allowed a more accurate and objective morpho-bathymetric description of the folds in map-view, and were used to extrapolate the morpho-structures identified in the seismic sections (Esteban et al., 2017). The slope values are influenced by the resolution of the data used, with higher slope values in the areas of higher resolution (i.e. multi-beam data, Grohmann, 2015). The slopes values in the area range from 0° to more than 30°, but in the figures the range values are constrained up to 8°.

It was not possible to migrate the seismic profiles in depth due to the lack of velocity data. Profiles in depth presented by other authors (Koenitz et al., 2008; Foschi and Cartwright, 2016) were used to infer the inclination of the faults associated with the folds. Koenitz et al. (2008) used interval velocities for each sedimentary sequence (see their Table 1 for the values) for the time-to-depth conversion. Foschi and Cartwright (2016) used velocity stack data to perform time-to-depth conversion.

In the seismic profiles presented in the corresponding figures, an axis with the approximate depth calculated with a speed of 1500 m/s, was added. The bathymetry and

slope data (calculated from the grid) were integrated to facilitate the identification and correlation of the morpho-bathymetric features.

The correlation of the geological units of the area was based on: (1) the geological information of the adjacent areas of Tierra del Fuego, Isla de Los Estados, Islas Malvinas/Falkland and the North Scotia Ridge (see Fig. 1), (2) the previous published seismic lines, (3) the observed seismic attributes, and (4) the morpho-bathymetric characteristics derived from the bathymetric and slope maps.

Five seismic units based on their geometric patterns, architecture, stratigraphic relationships, and regional unconformities were defined in this work (Table 1). The units B1 and B2 were recognized in the southern sector (Burdwood Bank and Terrace) and their speculative age is defined after Parker et al. (1996) and a geologic correlation with the outcrops in the North Scotia Ridge. The age of the units in the Malvinas/Falkland Trough sector (M1-M3) was constrained based on the core/well data. The age of the unit M1 is Mesozoic, according to Foschi and Cartwright (2016). The age of the units M2 and M3 are later discussed. The units M2 and M3 are both Cenozoic in age based on the well data (Foschi and Cartwright, 2016; Foschi et al., 2019) and were defined in relationship to deformation of the sequences of the Malvinas/Falkland Trough. The Unit M2 is pre-deformational while M3 is syn- and post-deformational.

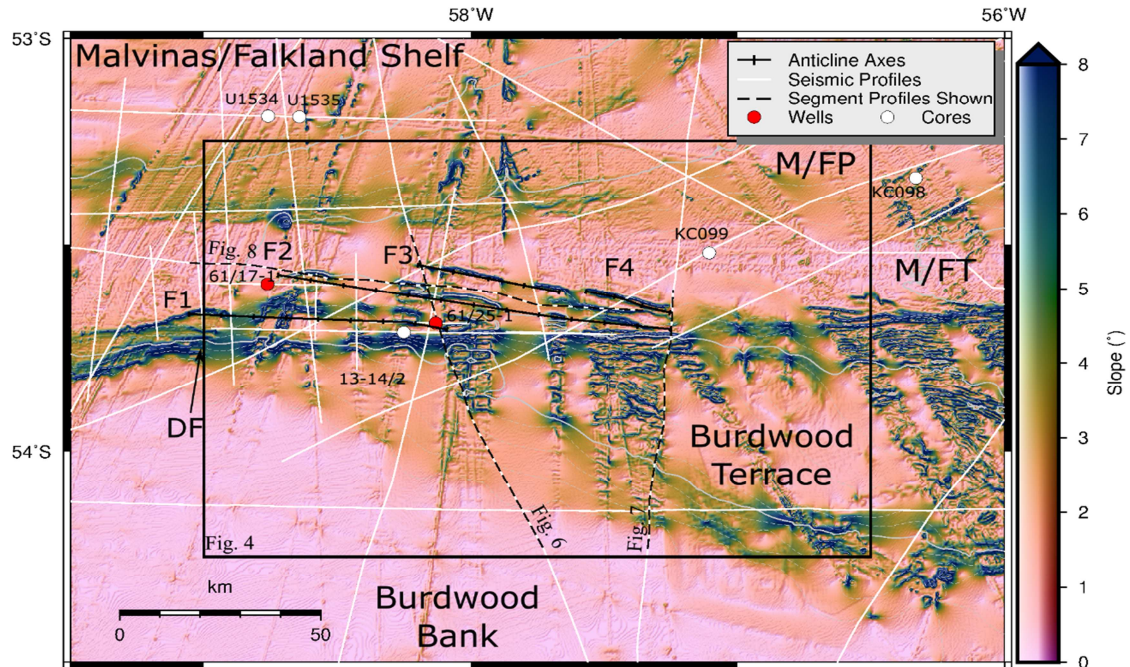
4 Results

4.1 Morphology of the folds

The folds here studied are located in the Malvinas/Falkland Trough, adjacent to the Burdwood Terrace and the Burdwood Bank. Their description is based on the morphology of the seabed revealed by bathymetric (Fig. 2) and slope data (Fig. 3), and its correlation with the seismic profiles (see Esteban et al. (2017) for a general description of the principal morpho-bathymetric units (Burdwood Bank, Burdwood Terrace, Malvinas/Falkland Shelf, Malvinas/Falkland Plateau)).

The folds of the Malvinas/Falkland Trough are located in the central sector (between *ca.* 57° W and 59° W) and they are developed in an area that has a triangular shape in map view, extending ~100 km in the E-W direction and ~16 km in the N-S direction (Figs. 4 and 5). Four parallel asymmetric folds that develop to progressively greater depths towards the north, with orientations ESE-WNW and lengths that vary between 22 and 98 km, were identified (Table 3). Their frontal limbs are steeper with slopes towards the NNE of *ca.* 4-6° and up to 10°, while the dorsal limbs have gentler slopes towards the SSW (*ca.* 3-4°; Fig. 3). Southwards, the

314 folds terminate against the abrupt E-W slope ($>4^\circ$) that corresponds to the limit with the
 315 Burdwood Bank and the Burdwood Terrace. Northwards the folds pass transitionally towards
 316 the low slope areas of the Malvinas/Falkland Trough.



318 Figure 3: Slope map of the Malvinas/Falkland Trough (M/FT) elaborated from the bathymetric
 319 grid DBM-BATDRAKE (Bohoyo et al., 2019) which has a grid resolution of 200 m, and combined
 320 multi-beam and satellite data (see text for more details). The deformation front (DF) of the
 321 thick-skinned fold-and-thrust Belt is shown. M/FP: Malvinas/Falkland Plateau.

322
 323 The northern edge of the Burdwood Terrace presents differences in its morphology
 324 along the E-W direction. In the western sector (up to $ca. 56.5^\circ$ W), in the area of the folds, it
 325 constitutes a structural high between the Burdwood Bank and the Malvinas/Falkland Trough
 326 (Fig. 6). In contrast, in the eastern sector there is a progressive deepening of the seafloor (Fig.
 327 4), resulting in a geometry of a typical accretion prism (see profile 144 of Ludwig and
 328 Rabinowitz, 1982; Westbrook et al., 1988). These differences can also be seen in the steep E-W
 329 slope of $ca. 110$ km of the deformation front where the slope decreases from W to E (DF in
 330 Figs. 4 and 5).

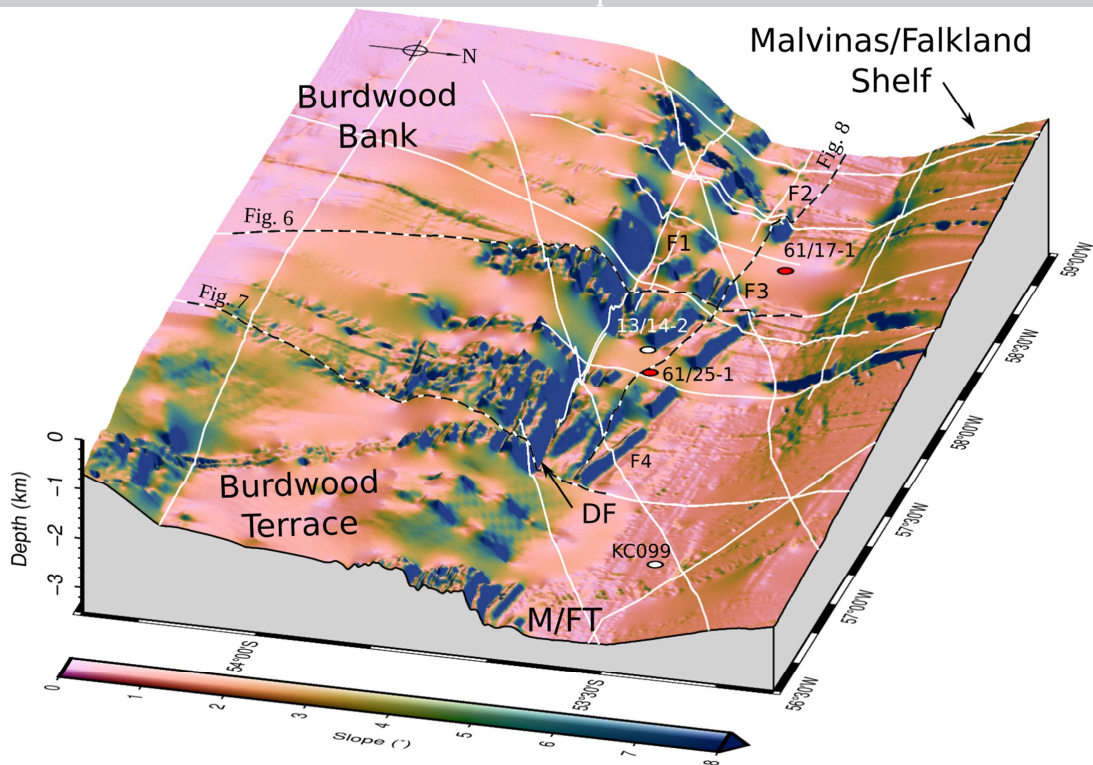


Figure 4: 3-D view of the Malvinas/Falkland Trough (M/FT) from the northeast. The figure is made from the bathymetric grid (source: DBM-BATDRAKE; Bohoyo et al., 2019; grid resolution of 200 m) with the slope map superimposed. The folds (F1 to F4) are located north of the Burdwood Bank and have WNW-ESE orientations.

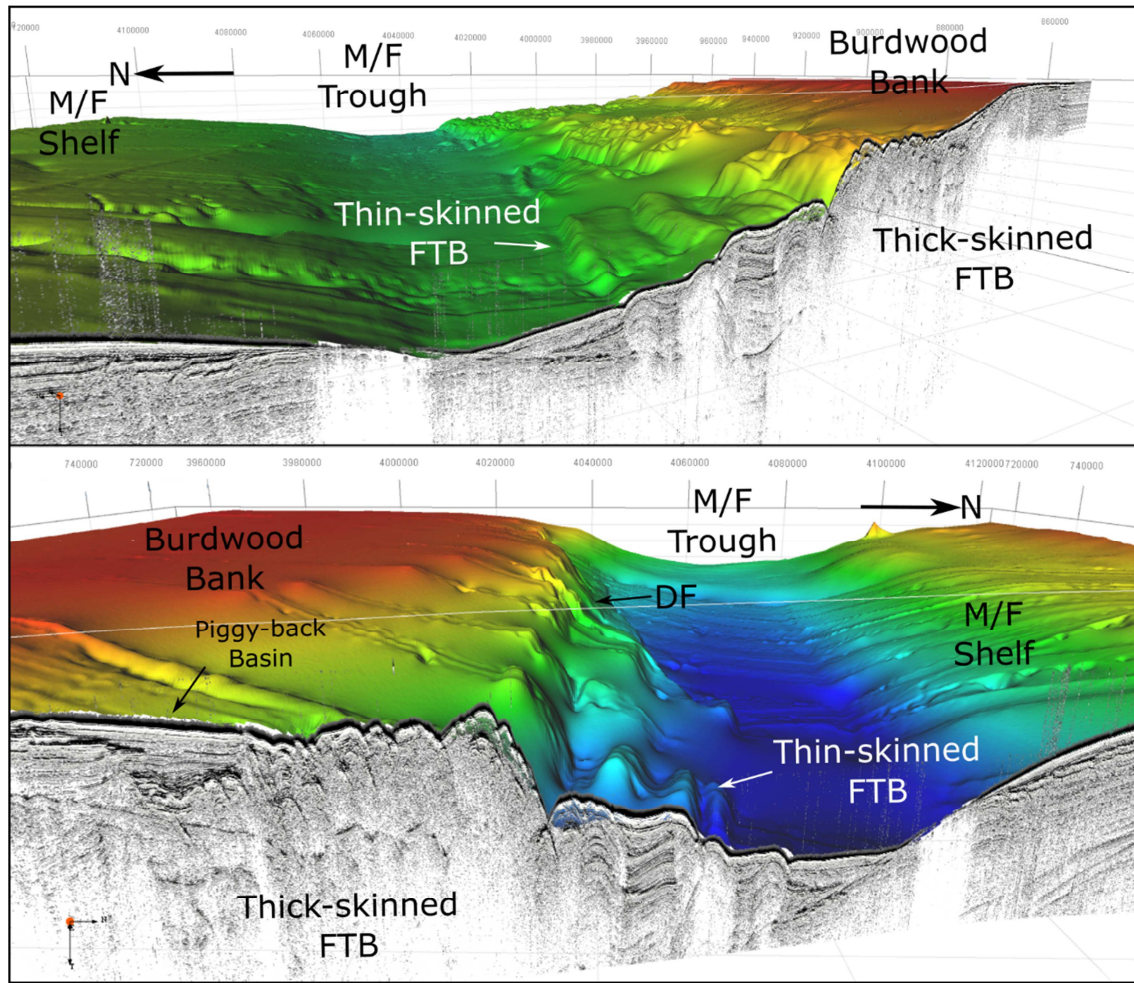


Figure 5: 3-D view of the Malvinas/Falkland (M/F) Trough from the W (top) and E (bottom) of the RC2106-145 seismic profile, integrated with the bathymetric data (source: DBM-BATDRAKE, Bohoyo et al., 2019, resolution of 200 m). The seismic profile was converted to depth with a speed of 1500 m/s (assumed). It shows the correlation of the main morpho-bathymetric units and their expression in the seismic profile (see Fig. 6 for its interpretation). The thick- and thin-skinned fold-and-thrust belts (FTB) were defined based on the involvement (or not) of the basement in the deformation after Bry et al. (2004). DF: Deformation Front.

# Fold	Length (km)	Axis (°)	Water Depth (m)
F1	64	94	2592-2612
F2	98	99	2280-2577
F3	36	102	2076-2198
F4	22	108	1616-1898

Table 3: Size of the identified folds of the Malvinas/Falkland Trough from S to N.

4.2 Seismic interpretation

4.2.1 Seismic Units

Unit B1 corresponds to the acoustic basement and is characterized by discontinuous reflectors of medium to low amplitude and low frequency, which result in a chaotic configuration (Fig. 6). Unit B2, developed over Unit 1, is composed of parallel reflectors between them and with the seabed, with high continuity and inclination to the north. It defines an infill basin deposit.

Unit M1 is located in the area of the South Malvinas/Falkland Basin, and is characterized by parallel reflectors of high lateral continuity and variable amplitude that incline southwards. This unit is correlated with the Mesozoic units of the South Malvinas/Falkland Basin (Bry et al., 2004; Fish, 2005; Foschi and Cartwright, 2016).

Unit M2 overlies Unit M1. It is composed of parallel reflectors with high lateral continuity, variable amplitude, high frequency and generally is parallel to the seabed. In some sectors the reflectors have very low amplitude. In other sectors, reflector packages of laminar shape and chaotic appearance are observed, interpreted as mass transport deposits (MTD, Foschi et al., 2019). This unit was identified by other authors (Bry et al., 2004; Fish, 2005; Ghiglione et al., 2010; Foschi et al., 2019). It correlates with units I and II of Koenitz et al. (2008). In the anticlines, eroded reflectors are observed (Foschi et al., 2019).

Unit M3 conformably overlies Unit M2. It is characterized by reflectors of high amplitude and lateral continuity with a basin infill geometry. Within the thin-skinned FTB it develops in the synclinals of the folds and presents evidence of growth strata (Fish, 2005; Ghiglione et al., 2010). It corresponds to the mini-basins described by Foschi et al. (2019). In the Malvinas/Falkland Trough area the unit has more extensive deposits interbedded with numerous MTDs (Foschi and Cartwright, 2016; Foschi et al., 2019) and correlates with units III and IV of Koenitz et al. (2008). The whole unit corresponds to the Fill Post Foreland of Fish (2005). In this unit the 2 m long core 13-14/2 (Cusminsky, 1991; Rivas et al., 2018) was recovered, which contains Holocene-Pleistocene foraminifera (Table 1).

4.2.2 Profile RC2106-145

Profile RC2106-145 has an NW-SE orientation and extends between Burdwood Bank, Burdwood Terrace and Malvinas/Falkland Trough (Figs. 5 and 6). It has been used to describe the regional framework of the area. It crosses obliquely the folds 1 to 3 (ca. 60°). The line

section between 0 and 16 km corresponds to the northern sector (southern on Fig. 6) of
 Burdwood Bank and Unit B1 presents horizontal reflectors in the shallowest sector. At greater
 depths there are numerous multiples (up to 6) that mask the seismic signal. This sector
 corresponds to the flat areas of Burdwood Bank. Between the 16 and 44 km is the transition
 between the Burdwood Bank and the Burdwood Terrace. Unit B2 outcrops and corresponds to
 the smooth seabed that deepens northwards. Between 44 and 62 km is found the Burdwood
 Terrace, characterized by a rough seabed, and its boundary with the Malvinas/Falkland
 Trough, which corresponds to the thick-skinned FTB described by Bry et al. (2004). In the
 seismic profile, Unit B1 is identified. The northern edge of the Burdwood Terrace (km 62)
 corresponds to the abrupt slope ($> 14^\circ$) of E-W direction (Figs. 4 to 6). Between 62 and 82 km,
 the line crosses folds 1 and 3. Internally, units M1 to M3 are identified. Unit M1 correlates with
 the Mesozoic sequences described by Bry et al. (2004); Koenitz et al. (2008); Foschi and
 Cartwright (2016). Above, within the folds 1 and 3 Unit M2 is identified (Figs. 5 and 6). This
 sector corresponds to the thin-skinned FTB described by Bry et al. (2004). To the north in the
 Malvinas/Falkland Trough (between 82 and 89 km) Unit M2 has horizontal reflectors and does
 not show deformation. Unit M3 is identified filling the syncline between the folds within the
 thin-skinned FTB.

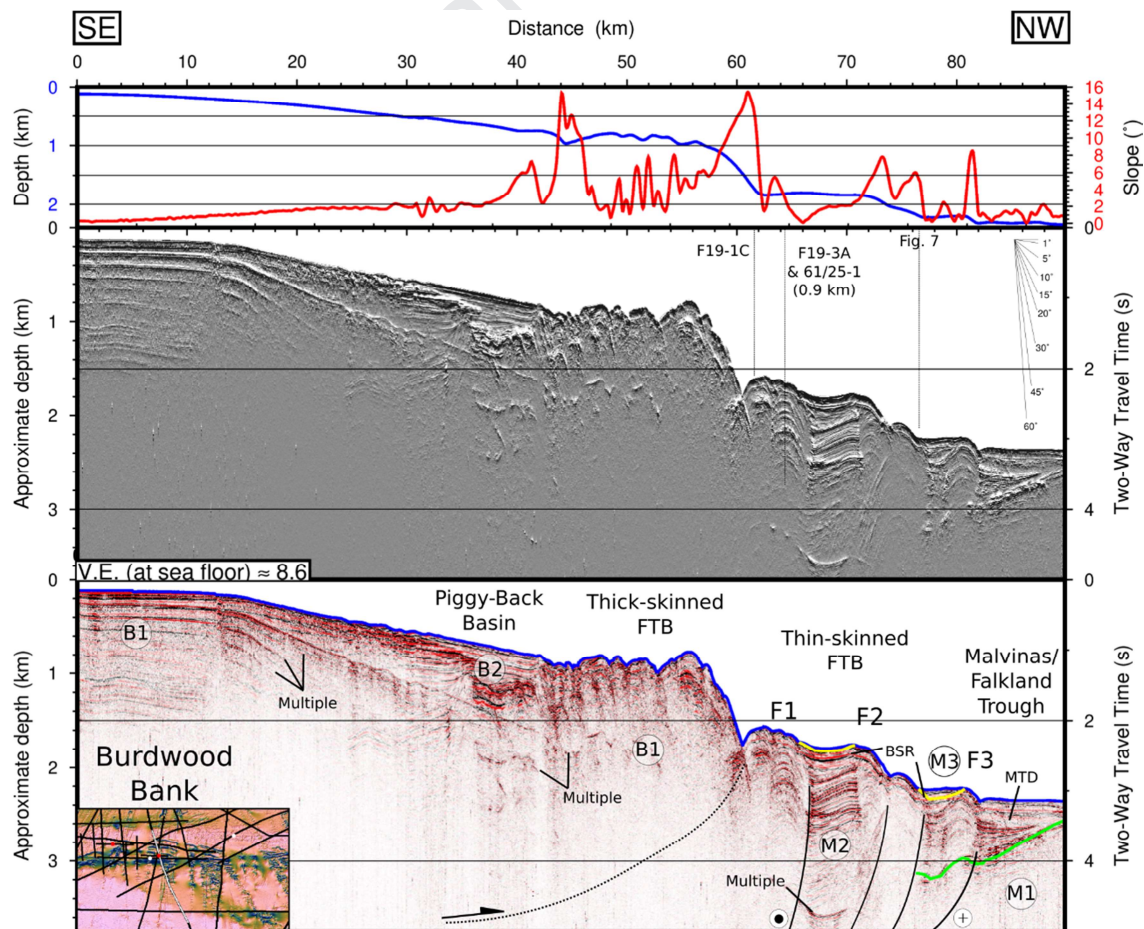


Figure 6: Bathymetric (blue) and slope (red) profiles (up) over the multi-channel seismic profile RC2106-145 (middle) processed with TecVA (Bulhões and de Amorim, 2005) and interpretations (below) across the Malvinas/Falkland Trough and with intersection with figures from Foschi et al. (2019; F19). Location in Fig. 2. The folds 1 to 3 (F1-F3) are located north of the Burdwood Bank and their reflectors can be followed undeformed into the Malvinas/Falkland Trough. MTD: Mass transport deposit. BSR: Bottom-simulating reflector. FTB: Fold-and-Thrust Belt. Seismic units (in circles) as Table 1.

4.2.3 Profile 77-26A

Seismic profile 77-26 has an N-S orientation and extends from the Burdwood Bank to the Malvinas/Falkland Trough (Fig. 7). It is located in the eastern end of the folds and runs across the folds 3 and 4. The same units present in the profile RC2106-145 have been identified: the northern edge of the Burdwood Bank with Unit B1 (from 0 to 5 km), a gentle slope with the unit B2 (from 5 to 30 km), the Burdwood Terrace again with the unit B1 (from 30 to 56 km) which ends in an abrupt slope up to 25° (58 km). Between 59 and 63 km, the line crosses the eastern end of the folds 3 and 4, where units M2 and M3 are identified. To the north in the Malvinas/Falkland Trough (from km 63 to 70), an incipient fold can be seen in depth, which is also identified further W in the profile 402 (see Richards et al., 1996; Bry et al., 2004).

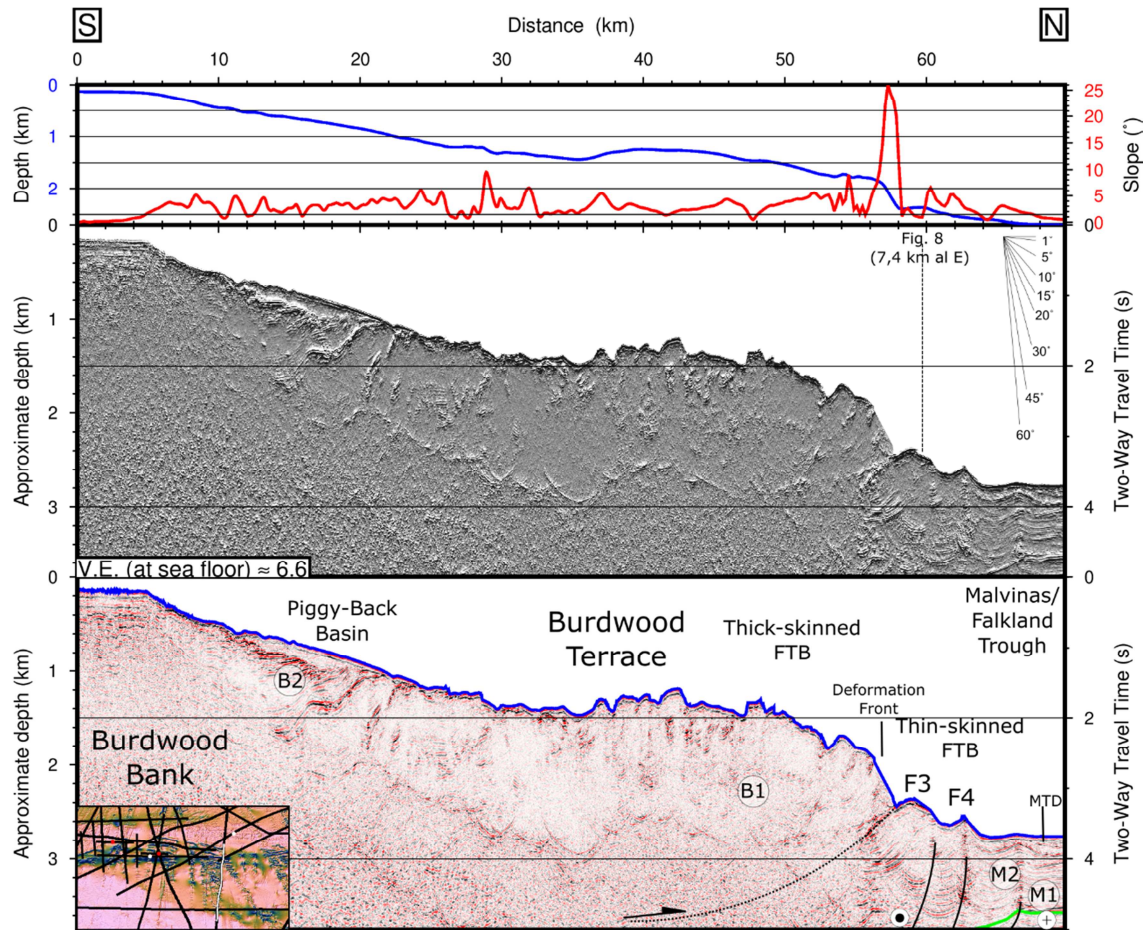


Figure 7: Bathymetric (blue) and slope (red) profiles (up) over the multi-channel seismic profile 77-26A (middle) processed with TecVA (Bulhões and de Amorim, 2005) and their interpretations (below). Location in Fig. 2. FTB: fold-and-thrust Belt. Seismic units (in circles) as Table 1.

4.2.4 Profile 77-20A

Seismic profile 77-20A (Fig. 8), located on the Malvinas/Falkland Trough, has an E-W orientation, and runs almost parallel to the axes of folds 2 to 4, which makes it difficult to analyze the geometry of these features. Unit M1 deepens slightly eastwards. In the western sector (between 0 and 28 km), Unit M2 is also identified. In the eastern sector (between 28 and 114 km) the reflectors identified in the western sector are still visible and are slightly folded. In the lower part (> 4 s TWT), the amplitude of the folds is smaller. At *ca.* 33 and 50 km two morphological highs are observed, which are located in the sectors where the fold 2 prosecutes further to the north (Fig. 4). Between *ca.* 100 and 110 km, Unit M3 is identified and presents a maximum thickness of 0.1 s TWT (*ca.* 220 m) filling a syncline between folds 3 and 4.

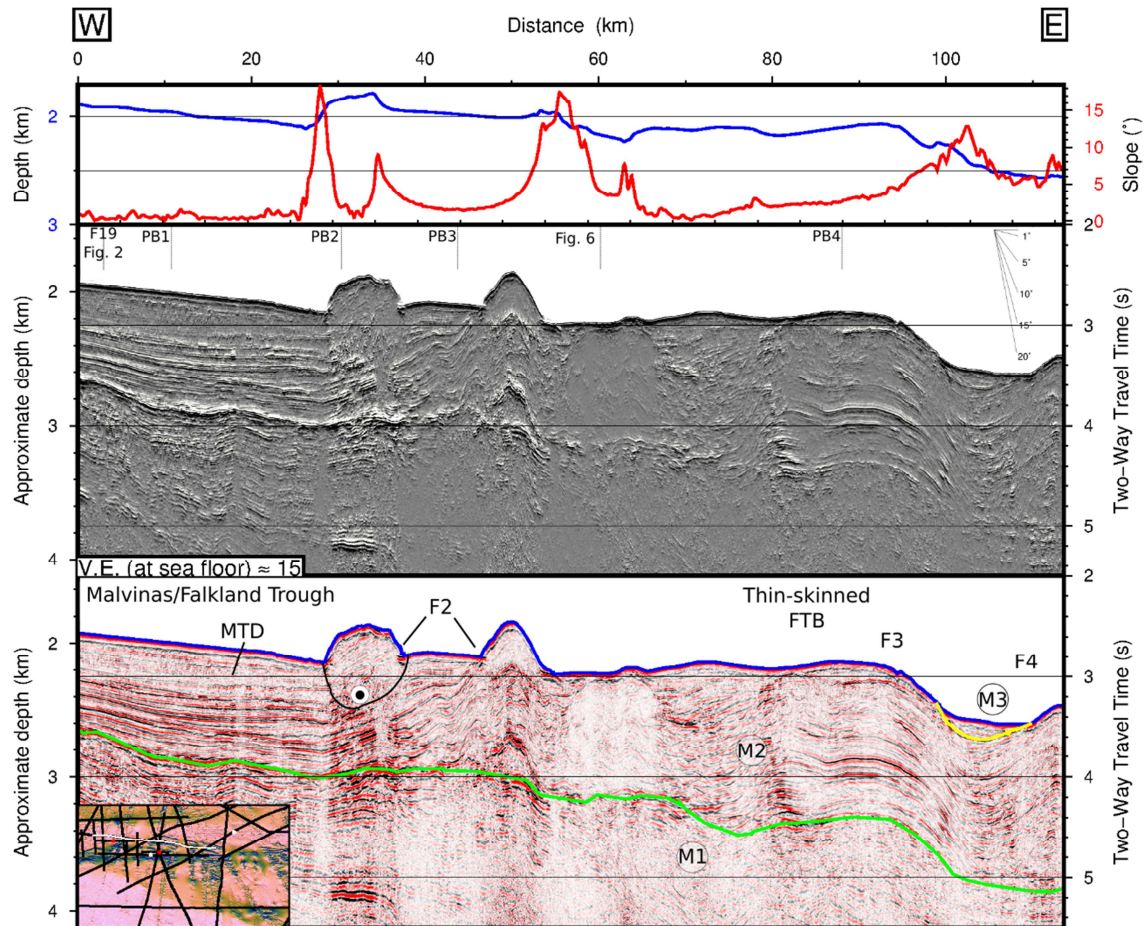


Figure 8: Bathymetric (blue) and slope (red) profiles (up) over the multi-channel seismic profile 77-20A (middle) processed with TecVA (Bulhões and de Amorim, 2005) and their interpretations (below). The profile runs along the Malvinas/Falkland Trough and is almost parallel to the axis of folds 2 and 3 (F2 and F3). Location in Fig. 2. The folds affected the sediments of the Malvinas/Falkland Trough. MTD: Mass transport deposit. FTB: Fold-and-Thrust Belt. Seismic units (in circles) as Table 1. PB1: Fig. 3 of Fish (2005) and Profile 1 of Koenitz et al. (2008). PB2: Profile 2 of Koenitz et al. (2008) and Fig. 3 of Bry et al. (2004). PB3: Fig. 5 of Fish (2005), Fig. 6 of Richards et al. (1996) and Fig. 5 of Platt and Philip (1995). PB4: Fig. 5B of Bry et al. (2004).

5 Discussion

5.1 Structural Map

Based on the interpretation and correlation of the data and its integration with previous maps (Tassone et al., 2008; Esteban, 2014; Esteban et al., 2018; Bohoyo et al., 2019; Foschi et al., 2019), a structural map of the seabed was elaborated for the area between the Burdwood Bank and the Malvinas/Falkland Shelf (Fig. 9).

The acoustic characteristics observed in the seismic profiles in the Burdwood Bank (unit B1) are similar to the units identified in the subsurface of the North Scotia Ridge (Cunningham, 1998; Tassone et al., 2008; Esteban et al., 2018; Ormazabal et al., 2019). This suggests that this bank is formed by Mesozoic units similar to the outcrops in the Fuegian Andes, Isla de Los Estados and in the Georgias Islands (Caminos and Nullo, 1979; Ponce and Martinez, 2007; Olivero and Malumián, 2008; Carter et al., 2014).

The area between the Burdwood Bank and the Burdwood Terrace is a smooth surface that extends in a WNW-ESE direction. It is constituted by piggy-back basins as previously indicated by Platt and Philip (1995), Parker et al. (1996), Bry et al. (2004), Fish (2005), filled with Paleogene sediments (unit B2 of Figs. 6 and 7). They probably constitute turbiditic deposits originated in the Burdwood Bank. Based on their tectonic origin, the piggy-back basins would have formed in the Oligocene-Miocene during the north migration of the Burdwood Bank (i.e. coeval with the compressive deformation).

To the north, the Burdwood Terrace area is characterized by a rough seabed with a progressive deepening towards the Malvinas/Falkland Trough (Figs. 2 and 3). It presents narrow basement ridges and incoherent reflectors (unit B1 in Figs. 6 and 7) previously described by Bry et al. (2004) as a thick-skinned FTB. These characteristics, added to the compressive tectonics, allow us to interpret it as an FTB that constitutes an accretion prism (or collision complex, according to Ludwig and Rabinowitz, 1982), where the sediments of the foreland (proto Malvinas/Falkland Trough) were continuously incorporated as the Burdwood Bank migrated northwards. This process allows us to interpret that the terrace is formed by older sediments near the Burdwood Bank that were first incorporated, and subsequently incorporated towards the Malvinas/Falkland Trough as the migration progressed. It is estimated that the outcrops age is Eocene?-Oligocene-Miocene. Based on the rough seafloor (Fig. 3) we may propose that no significant sedimentation has occurred. In areas with high-detailed bathymetry, linear features are observed (Figs. 3 and 9) that are interpreted as the axes of the folds of the accretion prism (see profile 144 of Ludwig and Rabinowitz, 1982). According to this interpretation, the axes are perpendicular to the compressional field that originated them. It is observed that there is a rotation of these lineaments towards the foreland, from 127° to the south, to *ca.* 90-100° to the north. This can be explained by a rotation of the Burdwood Bank (and its Terrace) during the northward migration of *ca.* 26° clockwise. The approach and collision of the Burdwood Bank with the Malvinas/Falkland Shelf could have caused this rotation. Similar structures were identified in Tierra del Fuego and Isla de Los Estados (Dalziel et al., 1974; Caminos and Nullo, 1979; Menichetti et al., 2008). It is

estimated that the differences in the morphology observed in the bathymetric data along the northern edge of the Burdwood Bank were formed from of an out-of-sequence thrust, probably due to the action of the basement of the Malvinas/Falkland Shelf as a tipping point (buttressing). Alternatively, this could be explained as an uplift associated with transpression as suggested by Ghiglione et al. (2010).

The lineaments of the Burdwood Terrace can be traced towards the E (*ca.* 54° W) with the NR1 lineament of Cunningham et al. (1998). This lineament shows similar characteristics in the seismic profiles (see both Figs. 7 of Cunningham et al., 1998; Ludwig and Rabinowitz, 1982). The NR1 lineament, located to the NW of the Bank Davis, has an ENE-WSW orientation. This broad difference in the orientation in contemporary structures could indicate that the Burdwood and Davis banks constitute two different blocks that moved independently to each other. It is estimated that the boundary between them could correspond to the Burdwood Lineament (which coincides in the Scotia Sea with the Burdwood Fracture Zone, Fig. 1; Esteban, 2014; Esteban and Tassone, 2017; Riley et al., 2019).

The thin-skinned FTB, as defined by Bry et al. (2004) is located north of the Burdwood Terrace and is comprised of the folds previously described (Table 3) that cover an area of *ca.* 100 x 16 km. These folds are controlled in general by sub-vertical faults (*ca.* 60°, measured in Fig. 2 of Foschi and Cartwright, 2016) with southward inclination to almost vertical (Fig. 1B of Foschi et al., 2019). Internally, they are composed of sediments similar to those present in the Malvinas/Falkland Trough (Figs. 6 and 8). These folds are interpreted as a positive flower structure (see below).

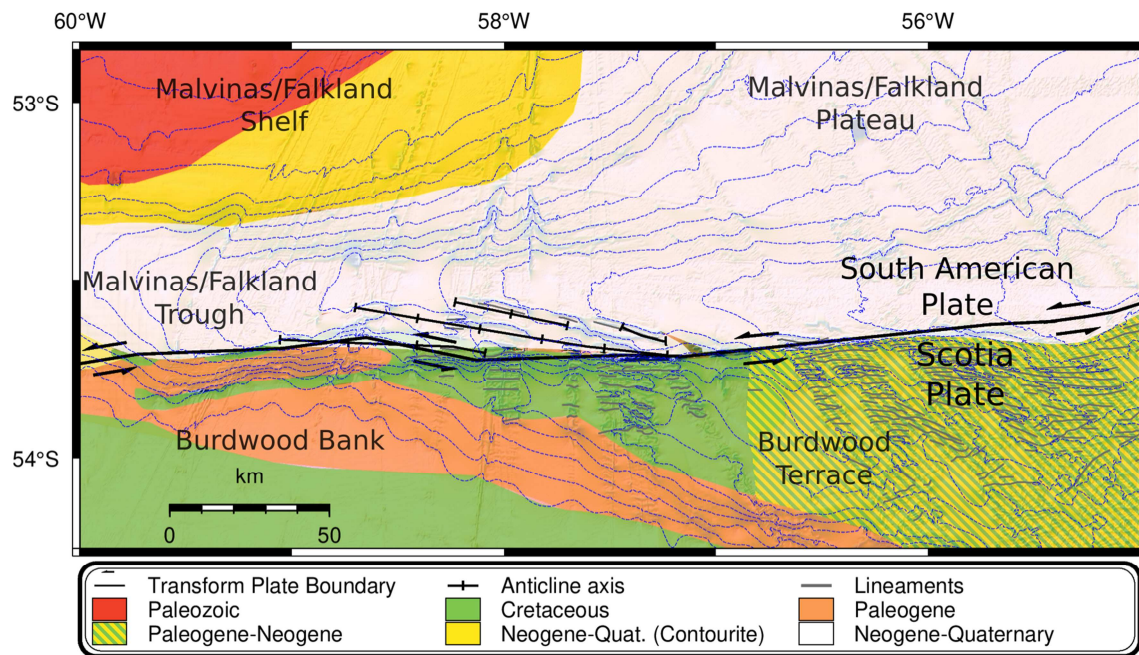


Figure 9: Geologic map of the offshore sector of the western Malvinas/Falkland Trough between Burdwood Bank and Malvinas/Falkland Shelf. Geological and structural data modified from Esteban (2014). Lineaments of the Burdwood Terrace map from Bohoyo et al. (2019). Contour lines every 200 m from DBM-BATHDRAKE grid.

5.2 Tectonic origin of the folds

The thin-skinned FTB presents different characteristics with respect to the thick-skinned FTB: that include the areal extension, orientation of the folds axes, internal structure, deformation age. These differences allow us to consider a different origin for each structure. In particular, the characteristics of the thin-skinned FTB are consistent with the left-lateral strike-slip tectonics that affected the region since the late Miocene (*ca.* 6-10 Ma, Lodolo et al. 2006; Torres Carbonell et al. 2014).

The areal extension of the structures is important to identify the tectonic style which originated them (Harding, 1985, 1990). The transpressive origin allows us to explain the areal extension of the thin-skinned FTB (*ca.* 100 km E-W and 16 km N-S). Changes in the orientation of the plate boundary with respect to the relative movement of the plates produce locally transpressive areas (such as the thin-skinned FTB) and transtensive areas (Sylvester, 1988; Cunningham and Mann, 2007). Towards the west, transtensive basins of late post-Miocene age (*ca.* 10 Ma) have been identified in the Malvinas/Falkland Basin (e.g. Western and Central Basins of Esteban et al., 2018) and in Tierra del Fuego (e.g., Lago Fagnano; Esteban et al., 2014) with sizes similar to the area covered by the thin-skinned FTB. Towards the east, Cunningham

et al. (1998) described seabed features (NR2c) identified as a modern deformation front. These structures (see their figure 7c) present characteristics similar to the thin-skinned FTB, so they could be interpreted as another local area of transpression associated with the current relative motion of the South American-Scotia plates.

The reinterpretation of the folds as transpressive structures indicates that N-S convergence has ceased in the Burdwood Bank area. This is coherent with the relict accretionary prism (NR1 lineaments) described to the east, which in some sectors is buried beneath undeformed sediments (Cunningham et al. 1998).

To explain the orientation of the axes folds, the theoretical model of the strike-slip structures is evaluated (Riedel, 1929; Sylvester, 1988; Dooley and Schreurs, 2012; Fig. 10). It is observed that they are coherent with the dominant left-lateral strike-slip tectonics in the region. In Fig. 10B, the stresses of the theoretical model are parallel to the relative movement between South America and Scotia plates (see displacement vectors from global inversion models in Fig. 10A). According to the theoretical model, the axes of the en-echelon folds have a theoretical orientation of 116° . Thus, there are differences between 22° to 8° with the observed fold axes (Table 3 and Fig. 10). Alternatively, if the theoretical model is rotated, so the en-echelon folds coincide with the folds identified in this work (Fig. 10C), it is observed that the left-lateral faults of the seabed (Foschi et al. 2019) coincide with the synthetic shear. In this case, the theoretical model predicts that the deformation stresses have an ENE-WSW direction (*ca.* 60°). In this way, the folds can be explained as positive flower structures (Sylvester, 1988; Dooley and Schreurs, 2012). A deviation is observed with respect to the Riedel shear model in the orientation of the fold axes from north to south (Table 3). This change would be explained as due to the greater influence that the previous structures have towards the south, conditioning the orientation of the fold axes, from an ENE-WSW trend to an E-W trend.

The interpretation of positive flower structures is consistent with the seismic profiles where it is observed that the deformation is concentrated in the upper units and decreases with depth (Richards et al., 1996; Fig. 8). Other important evidence is observed in depth-converted seismic profiles (Koenitz et al., 2008; Foschi and Cartwright, 2016), where the faults that control the folds reach inclinations of 60° , which is characteristic of strike-slip faults (see Sylvester, 1988). These inclinations are difficult to explain in thrusts in a compressive environment.

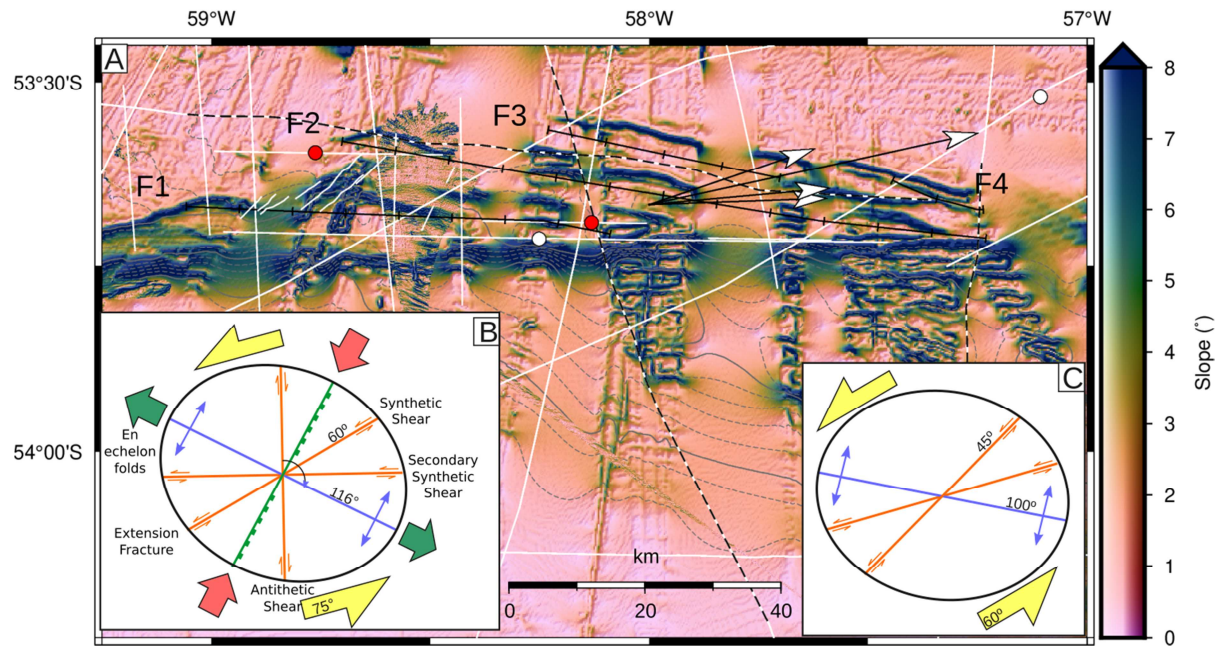


Figure 10: A) Slope map with the location of anticlinal axes (F1 to F4 from this work) and left-lateral faults (Foschi et al., 2019). Arrows indicate velocities of the Scotia Plate relative to the South America Plate from global inversion models calculated with Plate Motion Calculator (<https://www.unavco.org/software/geodetic-utilities/plate-motion-calculator/plate-motion-calculator.html>). B) Riedel model of a 75° (parallel to the white arrows) left-lateral simple shear with map-scale structures modified from Sylvester (1988). C) Simplified (60°) Riedel model with the structures identified in the area (en-echelon folds and synthetic shear).

The interpretation of the thin-skinned FTB as compressive structures (Ludwig and Rabinowitz, 1982; Platt and Philip, 1995) is difficult to support. This regime is contradicted by different authors who state that at that time the area was dominated by a left-lateral E-W strike-slip tectonics. On the one hand, the orientation of the fold axes would indicate a vergence towards the NNE (*ca.* 10°). That is a rotation of 10° with respect to the thick-skinned FTB (Fig. 4). Furthermore, it should be explained why this compressive activity developed locally (affecting an area of 100 km in the E-W direction) and did not spread more regionally. Particularly if we take into account that to the east, on the Malvinas/Falkland Trough, where there are undeformed Neogene sediments (Cunningham et al., 1998; Cunningham, 1998; Cunningham et al., 2002; Del Ben and Mallardi, 2004). In contrast, towards the west, transtensive basins were developed along the plate boundary (Lodolo et al., 2002, 2003; Tassone et al., 2005, 2008; Menichetti et al., 2008; Esteban et al., 2014, 2018).

5.3 Regional Implications

5.3.1 South Malvinas/Falkland Basin

The normal faulting of the sedimentary sequences of the South Malvinas/Falkland Basin provides evidence of the tectonic regime of the region. This faulting was caused by the flexure of the Malvinas/Falkland Shelf below the Burdwood Bank (Bry et al., 2004; Fish, 2005; Foschi and Cartwright, 2016).

Further to the north, within the contourite drift (Koenitz et al., 2008; Pérez et al., 2015), it is observed that normal faulting affected mainly its basal sequences (1A and 1B) with a middle Miocene (14.5 Ma) estimated age. This is consistent with a compressive regime due to a migration to the north of the Burdwood Bank, while the age of these deposits allows restricting this deformation to 14.5 Ma.

On the other hand, the upper units of the Contourite deposits (2A and 2B) do not show intense faulting. For this reason, it is inferred that coeval with this deposit, the migration to the north of the Burdwood Bank was much smaller. This is consistent with cessation of the compression at *ca.* 14 Ma (most likely due to the collision of the Burdwood Bank with the Malvinas/Falkland Shelf) and the beginning of a strike-slip regime as inferred by Koenitz et al. (2008). For the base of Unit 2A, Koenitz et al. (2008) estimated the maximum age of 9.5 Ma (late Miocene). These considerations about the faulting that affected the sedimentary sequence of the South Malvinas/Falkland Basin support the interpretation of a switch from a compressive regime to a transpressive one during the late Miocene (*ca.* 9.5 Ma). This age agrees with that proposed by Torres Carbonell et al. (2014) for the beginning of the Magallanes-Fagnano-Malvinas Fault System (*ca.* 10 Ma).

However, if we consider the new preliminary ages for the drift deposit (Weber et al., 2019), then the intense normal faulting occurred up to the late Pliocene-early Pleistocene (3.6-0.78 Ma; below reflector B in Table 1) when it decreased. This would indicate that the faulting is coeval with the strike-slip deformation. Since this regime is still active as revealed by GPS and earthquake data (Forsyth, 1975; Pelayo and Wiens, 1989; Thomas et al., 2003; Smalley et al., 2003, 2007; Costa et al., 2006; Mendoza et al., 2011, 2015), one can wonder about the change in the faulting intensity. One possibility is a general decrease in the velocity vector of the plates. Another possibility is a decreasing N-S velocity vector component, maybe caused by the buttressing effect due to the structural high of the Malvinas/Falkland Shelf.

5.3.2 Malvinas/Falkland Plateau

The structure of the Malvinas/Falkland Plateau is similar to that of the South Malvinas/Falkland Basin (Del Ben and Mallardi, 2004). These authors show that the F1 and F3 sequences were deformed and incorporated into the accretion prism (Table 1). Their ages

were calibrated with the DSDP 511 well and allow constraining the deformation event during the Paleocene-Miocene. However, the published seismic profile does not show enough details that could help to correlate it with one or both of the tectonic events (compression and transpression). Normal faulting (due to flexure of the plate) on the north flank of the Malvinas/Falkland Trough significantly affects the Cretaceous - Oligocene sequences (F1), while in the Miocene sequence (F3), the normal faulting is poorly developed. This would indicate that the compressional event for this sector lasted until the Oligocene - lower Miocene. On the other hand, towards the mid-Late Miocene, transpressive strike-slip tectonics prevailed, which considerably reduced the movement of the Burdwood Bank towards the north, and consequently the normal faulting of the northern flank. Based on this evidence, the deformation of the F1 and F3 sequences can be attributed to the compressional event.

6 Conclusions and evolutionary model

The fold-and-thrust Belt, located to the north of the Burdwood Bank, consists of both a thick-skinned and thin-skinned sections. The thick-skinned FTB is formed by Mesozoic units and originated by a compression towards the north during the Oligocene-late Miocene (*ca.* 28 - 7 Ma). The thin-skinned FTB developed in an area that extends *ca.* 100 km in the E-W direction and 16 km in the N-S direction between *ca.* 57° W and 59° W latitude. It consists of 4 parallel, asymmetric folds with ESE-WNW orientation and lengths ranging from 22 to 98 km. The folds affect Cenozoic sediments that are undeformed in the Malvinas/Falkland Trough. These folds have a late Miocene/Pliocene - Quaternary (post 7 Ma) age. They have been structured by the left-lateral strike-slip tectonic regime acting along the South American-Scotia plate boundary.

Based on the evidence presented in this work, the characteristics of each structure described, the deformation age of the units, and the bibliographic information on the surrounding areas, an evolutionary model of the area since the Oligocene is proposed (Fig. 11). The first phase, which includes the Oligocene-late Miocene (*ca.* 28-7 Ma), is characterized by the migration to the north of the Burdwood Bank, which originated the thick-skinned FTB and its associated piggy-back basins. During this migration the accretion prism of the Burdwood Terrace was generated. In this sector, the E-W trending lineaments shown in the bathymetric map are interpreted as relicts of this migration.

During the middle Miocene, with the onset of the Antarctic Intermediate Water, the sediments that constitute the lower units of the contourite initiated their deposition (Koenitz et al., 2008; Pérez et al., 2015). At the same time, as convergence progressed, the

Malvinas/Falkland Shelf (within the South American Plate) approached and begun to flex below the Burdwood Bank (Scotia Plate). This process originated the Malvinas/Falkland Trough (Cunningham et al., 1998) and produced an intense syn-tectonic normal faulting in the lower units of the contourite drift deposit in the South Malvinas/Falkland Basin (Bry et al., 2004; Koenitz et al., 2008). The sequences that constitute Unit M2 were deposited during this phase.

With the cessation of oceanic crust formation in the Scotia Plate during the late Miocene (7 Ma), the northward migration of the Burdwood Bank stopped while the sedimentation continued in the South Malvinas/Falkland Basin, and where minor normal faulting affected the upper units of the contourite drift deposit (Koenitz et al., 2008). The collision between the Burdwood Bank and the Malvinas/Falkland Shelf might have originated the steep deformation front of the thick-skinned FTB.

Finally, when left-lateral strike-slip tectonics initiated along the Malvinas/Falkland Trough (7-0 Ma), thin-skinned FTB originated and affected part of the sedimentary fill of the Malvinas/Falkland Trough. The M3 sequence deposited during this stage coeval with the deformation. This new tectonic regime originated the Mass Transport Deposits preserved in the sedimentary sequence. It is likely that previous structures developed during the compressive phase (which originated the thick-skinned FTB) were reactivated, as well as minor activity of the normal faults within the contourite drift.

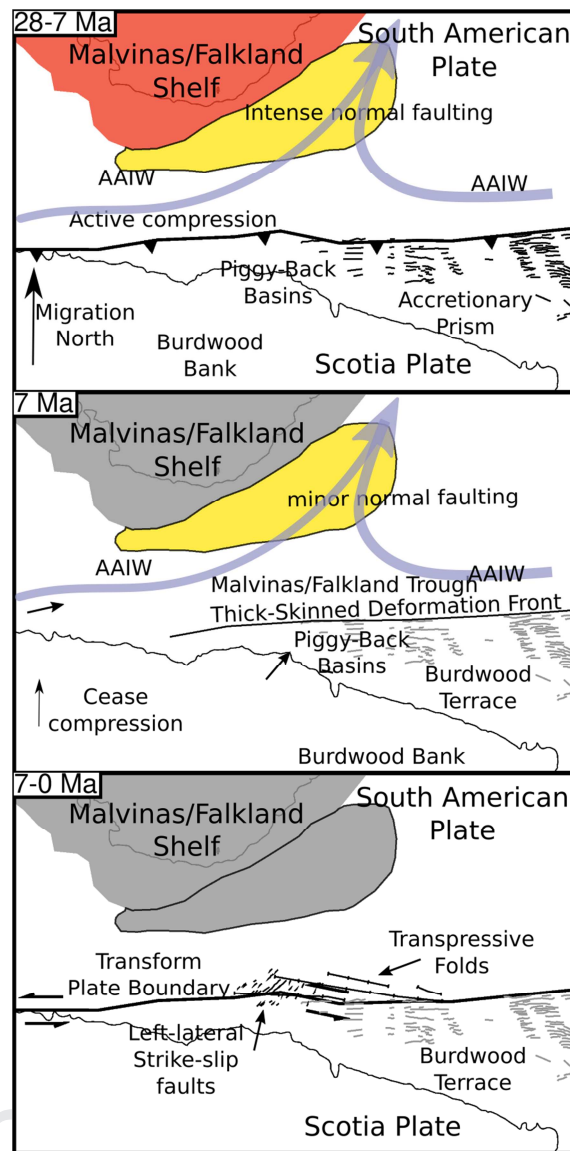


Figure 11: Evolutionary model of the Malvinas/Falkland Trough between the Burdwood Bank and the Malvinas/Falkland Shelf.

Acknowledgments

This contribution is framed within the “Pampa Azul” project, funded by the Secretary of Science Technology and Productive Innovation of Argentina. We are grateful for the constructive reviews by two anonymous reviewers and the Editor Dr. Andrés Folguera, which greatly helped to improve the original manuscript.

References

Baristeas, N., Anka, Z., di Primio, R., Rodriguez, J., Marchal, D., Dominguez, F., sep 2013. Newinsights into the tectono-stratigraphic evolution of the Malvinas Basin, offshore of the southernmostArgentinean continental margin. *Tectonophysics* 604, 280–295.

- 679 Barker, P. F., 2001. Scotia Sea regional tectonic evolution: implications for mantle flow and
680 palaeocirculation. *Earth-Science Reviews* 55 (1-2), 1–39.
- 681 Betka, P., Klepeis, K., Mosher, S., 2016. Fault kinematics of the Magallanes-Fagnano fault system,
682 southern Chile; an example of diffuse strain and sinistral transtension along a continental transform
683 margin. *Journal of Structural Geology* 85, 130–153.
- 684 Bohoyo, F., Larter, R. D., Galindo-Zaldívar, J., Leat, P. T., Maldonado, A., Tate, A. J., Flexas, M. M.,
685 Gowland, E. J. M., Arndt, J. E., Dorschel, B., Kim, Y. D., Hong, J. K., López-Martínez, J., Maestro, A.,
686 Bermúdez, O., Nitsche, F. O., Livermore, R. A., Riley, T. R., 2019. Morphological and geological features
687 of Drake Passage, Antarctica, from a new digital bathymetric model. *Journal of Maps* 15 (2), 49–59.
- 688 Bry, M., White, N., Singh, S., England, R., Trowell, C., 2004. Anatomy and formation of oblique
689 continental collision: South Falkland basin. *Tectonics* 23 (4), 1–20.
- 690 Bulhões, É. M., de Amorim, W. N., 2005. Princípio da Sismo Camada Elementar e sua aplicação à Técnica
691 Volume de Amplitudes (tecVA). In: 9th International Congress of the Brazilian Geophysical Society &
692 EXPOGEF, Salvador, Bahia, Brazil, 11-14 September 2005. Society of Exploration Geophysicists and
693 Brazilian Geophysical Society, pp. 1382–1387.
- 694 Caminos, R., Nullo, F., 1979. Descripción Geológica de la Hoja 67e, Isla de Los Estados. Tech. rep.,
695 Buenos Aires.
- 696 Carter, A., Curtis, M., Schwanethal, J., 2014. Cenozoic tectonic history of the South Georgia
697 microcontinent and potential as a barrier to Pacific-Atlantic through flow. *Geology* 42 (4), 299–302.
- 698 Costa, C. H., Smalley, R., Schwartz, D. P., Stenner, H. D., Ellis, M., Ahumada, E. A., Velasco, M. S., 2006.
699 Paleoseismic observations of an onshore transform boundary: The Magallanes-Fagnano fault, Tierra del
700 Fuego, Argentina. *Revista de la Asociacion Geologica Argentina* 61 (4), 647–657.
- 701 Cunningham, A. P., 1998. Geophysical Investigations of the North Scotia Ridge. Ph.D. thesis, University of
702 London.
- 703 Cunningham, A. P., Barker, P. F., 1996. Evidence for westward-flowing Weddell Sea Deep Water in the
704 Falkland Trough, western South Atlantic. *Deep Sea Research Part I: Oceanographic Research Papers* 43
705 (5), 643–654.
- 706 Cunningham, A. P., Barker, P. F., Tomlinson, J. S., 1998. Tectonics and sedimentary environment of the
707 North Scotia Ridge region revealed by side-scan sonar. *Journal of the Geological Society* 155 (6), 941–
708 956.
- 709 Cunningham, A. P., Howe, J. A., Barker, P. F., 2002. Contourite sedimentation in the Falkland Trough,
710 western South Atlantic. *Geological Society, London, Memoirs* 22, 337–352.

- 711 Cunningham, W.D., Mann, P., 2007. Tectonics of Strike-Slip Restraining and Releasing Bends, Geological
712 Society, London, Special Publications.
- 713 Cusminsky, G. C., 1991. Foraminíferos planctónicos de testigos Cenozoicos del océano Atlántico
714 sudoccidental austral. *Amegriniana* 28 (3-4), 225–240.
- 715 Dalziel, I. I. W. D., Caminos, R., Palmer, K. F., Nullo, F., Casanova, R., 1974a. South extremity of Andes:
716 Geology of Isla de los Estados, Argentine Tierra del Fuego. *The American Association of Petroleum*
717 *Geologists Bulletin* 58 (12), 2502–2512.
- 718 Dalziel, I. W., Lawver, L. a., Norton, I. O., Gahagan, L. M., 2013. The Scotia Arc: Genesis, Evolution, Global
719 Significance. *Annual Review of Earth and Planetary Sciences* 41 (1), 767–793.
- 720 Dalziel, I. W. D., de Wit, M. J., Palmer, K. F., 1974b. Fossil marginal basin in the southern Andes. *Nature*
721 250 (5464), 291–294.
- 722 Dalziel, I. W. D., Palmer, K. F., 1979. Progressive deformation and orogenic uplift at the southern
723 extremity of the Andes. *Bulletin of the Geological Society of America* 90 (3), 259–280.
- 724 Davey, F. J., 1972. Gravity measurements over Burdwood Bank. *Marine Geophysical Researches* 1, 428–
725 435.
- 726 Del Ben, A., Mallardi, A., 2004. Interpretation and chronostratigraphic mapping of multichannel seismic
727 reflection profile I95167, Eastern Falkland Plateau (South Atlantic). *Marine Geology* 209 (1-4), 347–361.
- 728 Dooley, T. P., Schreurs, G., 2012. Analogue modelling of intraplate strike-slip tectonics: A review and
729 new experimental results. *Tectonophysics* 574-575, 1–71.
- 730 Eagles, G., 2010. South Georgia and Gondwana's Pacific Margin: Lost in translation? *Journal of South*
731 *American Earth Sciences* 30 (2), 65–70.
- 732 Eagles, G., 2016. Tectonic Reconstructions of the Southernmost Andes and the Scotia Sea During the
733 Opening of the Drake Passage. In: *Geodynamic Evolution of the Southernmost Andes*. Springer
734 International Publishing, 75–108.
- 735 Eagles, G., Jokat, W., 2014. Tectonic reconstructions for paleobathymetry in Drake Passage.
736 *Tectonophysics* 611, 28–50.
- 737 Eagles, G., Livermore, R. A., Fairhead, J. D., Morris, P., 2005. Tectonic evolution of the west Scotia Sea.
738 *Journal of Geophysical Research B: Solid Earth* 110 (2), 1–19.
- 739 Espósito, G. J., 1981. Estudio sedimentológico de testigos verticales del Plateau de Malvinas, Margen
740 Continental Argentino. Tech. Rep.
- 741 Esteban, F., Tassone, A., Isola, J., Lodolo, E., Menichetti, M., 2018. Geometry and structure of the pull-
742 apart basins developed along the western South American-Scotia plate boundary (SW Atlantic Ocean).
743 *Journal of South American Earth Sciences* 83, 96–116.

- 744 Esteban, F. D., 2014. Estudio geofísico-geológico del subsuelo del segmento noroccidental de la Dorsal
745 Norte de Scotia. Argentina. Tesis. Ph.D. thesis, Universidad de Buenos Aires.
- 746 Esteban, F. D., Tassone, A., Lodolo, E., Menichetti, M., 2010. Morphostructure of the western sector of
747 the North Scotia Ridge. *Geosur* (1), 1–5.
- 748 Esteban, F. D., Tassone, A., Lodolo, E., Menichetti, M., 2012. The South America-Scotia plate boundary
749 from 67 °W to 56 °W (Southermost Atlantic ocean). *Rendiconti Online Societa Geologica Italiana* 22, 76–
750 79.
- 751 Esteban, F. D., Tassone, A., Lodolo, E., Menichetti, M., 2013. Structural setting of the western South
752 America-Scotia plate boundary. In: Lobo, F. J., Pèrez, L. F., Martos, Y. M. (Eds.), *The Scotia Arc:
753 Geodynamic Evolution & Global Implications*. Instituto Andaluz de Ciencias de la Tierra, Granada, 47–48.
- 754 Esteban, F. D., Tassone, A., Lodolo, E., Menichetti, M., Lippai, H., Waldmann, N., Darbo, A., Baradello, L.,
755 Vilas, J. F., 2014. Basement geometry and sediment thickness of Lago Fagnano (Tierra del Fuego).
756 *Andean Geology* 41 (2), 293–313.
- 757 Esteban, F. D., Tassone, A., Menichetti, M., Lodolo, E., 2017. Application of Slope Maps as a Complement
758 of Bathymetry: Example from the SW Atlantic. *Marine Geodesy* 40 (1), 57–71.
- 759 Esteban, F. D., Tassone, A., Menichetti, M., Rapalini, A. E., Remesal, M. B., Cerrredo, M. E., Lippai, H.,
760 Vilas, J. F., 2011. Magnetic fabric and microstructures across the Andes of Tierra del Fuego, Argentina.
761 *Andean Geology* 38 (1), 64–81.
- 762 Esteban, F. D., Tassone, A. A., 2017. Morfoestructuras y continuidad en la región de Tierra del Fuego y
763 Dorsal Norte de Scotia de lineamientos tectónicos asociados a la apertura de la Placa de Scotia. In:
764 *Congreso Geológico Argentino*. Tucuman, 12–13.
- 765 Farran, M., 2008. IMAGE2SEGY: Una aplicación informática para la conversión de imágenes de perfiles
766 sísmicos a ficheros en formato SEG Y. In: *VII Congreso Geológico de España*. Las Palmas de Gran
767 Canaria, 1–4.
- 768 Fish, P., 2005. Frontier South, East Falkland basins reveal important exploration potential. *Oil & Gas
769 Journal* 103 (45), 34–40.
- 770 Forsyth, D. W., 1975. Fault Plane Solutions and Tectonics of the South Atlantic and Scotia Sea. *Journal of
771 Geophysical Research* 80 (11), 1429–1443.
- 772 Foschi, M., Cartwright, J. A., 2016. South Malvinas/Falkland Basin: Hydrocarbon migration and
773 petroleum system. *Marine and Petroleum Geology* 77, 124–140.
- 774 Foschi, M., Paganoni, M., Cartwright, J., Idiz, E., 2019. Microbial vs thermogenic gas hydrates in the
775 South Falkland Basin: BSR distribution and fluid origin. *Marine and Petroleum Geology* 102, 695–703.

- 776 Galeazzi, J. S., 1998. Structural and Stratigraphic Evolution of the Western Malvinas Basin, Argentina.
777 AAPG Bulletin 82 (4), 596–636.
- 778 Ghiglione, M. C. (Ed.), 2016. Geodynamic Evolution of the Southernmost Andes. Springer Earth System
779 Sciences. Springer International Publishing, Cham.
- 780 Ghiglione, M. C., Quinteros, J., Yagupsky, D., Bonillo-Martínez, P., Hlebszevtich, J., Ramos, V. A., Vergani,
781 G., Figueroa, D., Quesada, S., Zapata, T., 2010. Structure and tectonic history of the foreland basins of
782 southernmost South America. *Journal of South American Earth Sciences* 29 (2), 262–277.
- 783 Giner-Robles, J. L., González-Casado, J. M., Gumiel, P., Martín-Velázquez, S., García-Cuevas, C., 2003. A
784 kinematic model of the Scotia plate (SW Atlantic Ocean). *Journal of South American Earth Sciences* 16
785 (4), 179–191.
- 786 Grohmann, C. H., 2015. Effects of spatial resolution on slope and aspect derivation for regional-scale
787 analysis. *Computers & Geosciences* 77, 111–117.
- 788 Hagelund, E. R., Levin, S. A., 2017. SEG-Y_r2.0: SEG-Y revision 2.0 Data Exchange format. Tech. Rep.
- 789 Harding, T. P., 1985. Seismic Characteristics and Identification of Negative Flower Structures, Positive
790 Flower Structures, and Positive Structural Inversion. AAPG Bulletin 69 (4), 582–600.
- 791 Harding, T. P., 1990. Identification of Wrench Faults Using Subsurface Structural Data: Criteria and
792 Pitfalls. AAPG Bulletin 74 (10), 1590–1609.
- 793 Hervé, F., Calderón, M., Fanning, M., Kraus, S., Pankhurst, R., 2010. SHRIMP chronology of the
794 Magallanes Basin basement, Tierra del Fuego: Cambrian plutonism and Permian high-grade
795 metamorphism. *Andean Geology* 37 (2), 253–275.
- 796 Herve, F., Fanning, C. M., Pankhurst, R. J., Mpodozis, C., Klepeis, K., Calderon, M., Thomson, S. N., 2010.
797 Detrital zircon SHRIMP U-Pb age study of the Cordillera Darwin Metamorphic Complex of Tierra del
798 Fuego: sedimentary sources and implications for the evolution of the Pacific margin of Gondwana.
799 *Journal of the Geological Society* 167 (3), 555–568.
- 800 Howe, J. A., Pudsey, C. J., Cunningham, A. P., 1997. Pliocene-Holocene contourite deposition under the
801 Antarctic Circumpolar Current, western Falkland Trough, south Atlantic Ocean. *Marine Geology* 138 (1-
802 2), 27–50.
- 803 Klepeis, K. A., 1994. The Magallanes and Deseado fault zones: Major segments of the South
804 AmericanScotia transform plate boundary in southernmost South America, Tierra del Fuego. *Journal of*
805 *Geophysical Research: Solid Earth* 99 (B11), 22001–22014.
- 806 Klepeis, K. A., Austin, J. A., 1997. Contrasting styles of superposed deformation in the southernmost
807 Andes. *Tectonics*. 16 (5), 755-776.

- 808 Koenitz, D., White, N., Nick McCave, I., Hobbs, R., 2008. Internal structure of a contourite drift generated
809 by the Antarctic Circumpolar Current. *Geochemistry, Geophysics, Geosystems* 9 (6), 1–27.
- 810 Livermore, R., Nankivell, A., Eagles, G., Morris, P., 2005. Paleogene opening of Drake Passage. *Earth and*
811 *Planetary Science Letters* 236 (1-2), 459–470.
- 812 Lodolo, E., Donda, F., Tassone, A., 2006. Western Scotia Sea margins: Improved constraints on the
813 opening of the Drake Passage. *Journal of Geophysical Research: Solid Earth* 111 (6), 1–14.
- 814 Lodolo, E., Menichetti, M., Bartole, R., Ben-Avraham, Z., Tassone, A., Lippai, H., 2003. Magallanes
815 Fagnano continental transform fault (Tierra del Fuego, southernmost South America). *Tectonics* 22 (6),
816 15–26.
- 817 Lodolo, E., Menichetti, M., Tassone, A., Geletti, R., Sterzai, P., Lippai, H., Hormaechea, J.-L., 2002.
818 Researchers target a continental transform fault in Tierra del Fuego. *Eos, Transactions American*
819 *Geophysical Union* 83 (1), 1.
- 820 Lovecchio, J. P., Naipauer, M., Cayo, L. E., Rohais, S., Giunta, D., Flores, G., Gerster, R., Bolatti, N. D.,
821 Joseph, P., Valencia, V. A., Ramos, V. A., 2019. Rifting evolution of the Malvinas basin, offshore
822 Argentina: New constrains from zircon U/Pb geochronology and seismic characterization. *Journal of*
823 *South American Earth Sciences* 95, 102253.
- 824 Ludwig, W. J., 1983. Geologic Framework of the Falkland Plateau. In: *Initial Reports of the Deep Sea*
825 *Drilling Project*, 71. U.S. Government Printing Office, Ch. 7, 281–293.
- 826 Ludwig, W. J., Rabinowitz, P. D., 1982. The collision complex of the North Scotia Ridge. *Journal of*
827 *Geophysical Research* 87 (B5), 3731–3740.
- 828 Malumián, N., Olivero, E. B., 2005. El Oligoceno-Plioceno marino del río Irigoyen, costa atlántica de
829 Tierra del Fuego, Argentina: una conexión atlántico-pacífica. *Revista geológica de Chile* 32 (1), 117–129.
- 830 Mendoza, L., Perdomo, R., Hormaechea, J. L., Cogliano, D. D., Fritsche, M., Richter, A., Dietrich, R., 2011.
831 Present-day crustal deformation along the Magallanes-Fagnano Fault System in Tierra del Fuego from
832 repeated GPS observations. *Geophysical Journal International* 184 (3), 1009–1022.
- 833 Mendoza, L., Richter, A., Fritsche, M., Hormaechea, J. L., Perdomo, R., Dietrich, R., 2015. Block modeling
834 of crustal deformation in Tierra del Fuego from GNSS velocities. *Tectonophysics* 651, 58–65.
- 835 Menichetti, M., Lodolo, E., Tassone, A., 2008. Structural geology of the Fuegian Andes and Magallanes
836 fold-and-thrust belt - Tierra del Fuego Island. *Geologica Acta* 6 (1), 19–42.
- 837 Nelson, E. P., Dalziel, I. W. D., Milnes, A. G., 1980. Structural geology of the Cordillera Darwin -
838 collisional-style orogenesis in the southernmost Chilean Andes. *Eclogae geologicae Helvetiae* 73 (3),
839 727–751.

- 840 Olivero, E. B., Malumián, N., 2008. Mesozoic-Cenozoic stratigraphy of the Fuegian Andes, Argentina.
841 *Geologica Acta* 6 (1), 5–18.
- 842 Olivero, E. B., Martinioni, D. R., 2001. A review of the geology of the Argentinian Fuegian Andes. *Journal*
843 *of South American Earth Sciences* 14 (2), 175–188.
- 844 Onorato, M.R., Perucca, L., Coronato, A., Rabassa, J., López, R., 2016. Seismically-induced soft-sediment
845 deformation structures associated with the Magallanes–Fagnano Fault System (Isla Grande de Tierra del
846 Fuego, Argentina). *Sediment. Geol.* <https://doi.org/10.1016/j.sedgeo.2016.04.010>
- 847 Ormazabal, J. P., Tassone, A., Esteban, F., Isola, J., Cayo, L. E., Lozano, J., Menichetti, M., Lodolo, E.,
848 2019. Structure of the wedge-top and foredeep of the Magallanes-Malvinas basins between 62° W and
849 67° W (SW Atlantic Ocean). *Journal of South American Earth Sciences* 93, 364–381.
- 850 Parker, G., Violante, R., Paterlini, M., 1996. Fisiografía de la plataforma continental. In: Ramos, V.A.,
851 Turic, M. (Eds.), *Geología y Recursos Naturales de la Plataforma Continental Argentina*. XIII Congreso
852 Geológico Argentino; III Congreso de Exploración de Hidrocarburos. Buenos Aires, 1–16.
- 853 Pelayo, A. M., Wiens, D. A., 1989. Seismotectonics and relative plate motions in the Scotia Sea region.
854 *Journal of Geophysical Research* 94 (B6), 7293–7320.
- 855 Pérez, L. F., Bohoyo, F., Hernández-Molina, F. J., Casas, D., Galindo-Zaldívar, J., Ruano, P., Maldonado, A.,
856 2016. Tectonic activity evolution of the Scotia-Antarctic Plate boundary from mass transport deposit
857 analysis. *Journal of Geophysical Research: Solid Earth* 121 (4), 2216–2234.
- 858 Pérez, L. F., Hernández-Molina, F. J., Esteban, F. D., Tassone, A., Piola, A. R., Maldonado, A., Preu, B.,
859 Violante, R. A., Lodolo, E., 2015. Erosional and depositional contourite features at the transition
860 between the western Scotia Sea and southern South Atlantic Ocean: links with regional water-mass
861 circulation since the Middle Miocene. *Geo-Marine Letters* 35 (4), 271–288.
- 862 Platt, N. H., Philip, P. R., 1995. Structure of the southern Falkland Islands continental shelf: initial results
863 from new seismic data. *Marine and Petroleum Geology* 12 (7), 759–771.
- 864 Ponce, J. F., Martinez, O., 2007. Hallazgo de depósitos sedimentarios postcretácicos en Bahía Crossley,
865 Isla de los Estados, Tierra del Fuego. *Revista de la Asociacion Geologica Argentina* 62 (3), 467–470.
- 866 Raggio, F., Welsink, H., Fiptiani, N., Prayitno, W., Gerster, R., 2011. Cuenca Malvinas. In: VIII Congreso de
867 Exploración y Desarrollo de Hidrocarburos Simposio Cuencas Argentinas: visión actual. 1–16.
- 868 Richards, P. C., Gatliff, R. W., Quinn, M. F., Fannin, N. G. T., Williamson, J. P., 1996. The geological
869 evolution of the Falkland Islands continental shelf. *Geological Society, London, Special Publications* 108
870 (1), 105–128.
- 871 Riedel, W., 1929. Zur mechanik geologischer Brucherscheinungen. *Zentralblatt für Mineralogie*,
872 *Geologie und Paläontologie*, 354–368.

- 873 Riley, T. R., Carter, A., Leat, P. T., Burton-Johnson, A., Bastias, J., Spikings, R. A., Tate, A. J., Bristow, C. S.,
874 2019. Geochronology and geochemistry of the northern Scotia Sea: A revised interpretation of the North
875 and West Scotia ridge junction. *Earth and Planetary Science Letters* 518, 136–147.
- 876 Rivas, L., Pérez Panera, J. P., Cusminsky, G. C., 2018. Pliocene - Holocene calcareous nannofossils from
877 the Malvinas Trough, southwestern Atlantic Ocean. In: *Reunión de Comunicaciones de la Asociación*
878 *Paleontológica Argentina*. Puerto Madryn, 92.
- 879 Rossello, E. A., 2005. Kinematics of the Andean sinistral wrenching along the Fagnano-Magallanes fault
880 zone (Argentina-Chile Fuegian foothills). In: *International Symposium of Andean Geodynamics*. 623–626.
- 881 Ryan, W.B.F., Carbotte, S.M., Coplan, J.O., O'Hara, S., Melkonian, A., Arko, R., Weissel, R.A., Ferrini, V.,
882 Goodwillie, A., Nitsche, F., Bonczkowski, J., Zemsky, R., 2009. Global multi-resolution topography
883 synthesis. *Geochemistry, Geophys. Geosystems* 10. <https://doi.org/10.1029/2008GC002332>
- 884 Smalley, J., Dalziel, I. W. D., Bevis, M. G., Kendrick, E., Stamps, D. S., King, E. C., Taylor, F. W., Lauría, E.,
885 Zakrajsek, A., Parra, H., 2007. Scotia arc kinematics from GPS geodesy. *Geophysical Research Letters* 34
886 (21), 1–6.
- 887 Smalley, R., Kendrick, E., Bevis, M. G., Dalziel, I. W. D., Taylor, F., Lauría, E., Barriga, R., Casassa, G.,
888 Olivero, E., Piana, E., 2003. Geodetic determination of relative plate motion and crustal deformation
889 across the Scotia-South America plate boundary in eastern Tierra del Fuego. *Geochemistry, Geophysics,*
890 *Geosystems* 4 (9), 1–19.
- 891 Stone, P., 2016. Geology reviewed for the Falkland Islands and their offshore sedimentary basins, South
892 Atlantic Ocean. *Earth and Environmental Science Transactions of the Royal Society of Edinburgh* 106
893 (02), 115–143.
- 894 Sylvester, A. G., 1988. Strike-slip faults. *Geological Society of America Bulletin* 100 (11), 1666–1703.
- 895 Tassone, A., Lippai, H., Lodolo, E., Menichetti, M., Comba, A., Hormaechea, J. L., Vilas, J. F., 2005. A
896 geological and geophysical crustal section across the Magallanes-Fagnano fault in Tierra del Fuego.
897 *Journal of South American Earth Sciences* 19 (1 SPEC. ISS.), 99–109.
- 898 Tassone, A., Lodolo, E., Menichetti, M., Yagupsky, D., Vilas, J. F., 2008. Seismostratigraphic and structural
899 setting of the Malvinas Basin and its southern margin (Tierra del Fuego Atlantic offshore). *Geologica*
900 *Acta* 6 (1), 55–67.
- 901 Thomas, C., Livermore, R., Pollitz, F., 2003. Motion of the Scotia sea plates. *Geophysical Journal*
902 *International* 155 (3), 789–804.
- 903 Torres Carbonell, P. J., Dimieri, L. V., Olivero, E. B., Bohoyo, F., Galindo-Zaldívar, J., 2014. Structure and
904 tectonic evolution of the Fuegian Andes (southernmost South America) in the framework of the Scotia
905 Arc development. *Global and Planetary Change* 123, 174–188.

- 906 Torres Carbonell, P. J., Olivero, E. B., Dimieri, L. V., 2008. Control en la magnitud de desplazamiento de
907 rumbo del Sistema Transformante Fagnano, Tierra del Fuego, Argentina. *Revista Geologica de Chile* 35
908 (1), 63–77.
- 909 Uliana, M. A., Biddle, K. T., Cerdan, J., 1989. Mesozoic Extension and the Formation of Argentine
910 Sedimentary Basins. In: *Extensional Tectonics and Stratigraphy of the North Atlantic Margins*. Ch. 39,
911 599–614.
- 912 V  rard, C., Flores, K., Stampfli, G., 2012. Geodynamic reconstructions of the South America - Antarctica
913 plate system. *Journal of Geodynamics* 53 (1), 43–60.
- 914 Weber, M., Raymo, M., Peck, V., Williams, T., 2019. Expedition 382 Preliminary Report: Iceberg Alley and
915 Subantarctic Ice and Ocean Dynamics. Vol. 382 of *International Ocean Discovery Program Preliminary*
916 *Report*. International Ocean Discovery Program.
- 917 Wessel, P., Smith, W. H. F., Scharroo, R., Luis, J., Wobbe, F., 2013. Generic Mapping Tools: Improved
918 Version Released. *Eos, Transactions American Geophysical Union* 94 (45), 409–410.
- 919 Westbrook, G. K., Ladd, J. W., Buhl, P., Bangs, N., Tiley, G. J., 1988. Cross section of an accretionary
920 wedge: Barbados Ridge complex. *Geology* 16 (7), 631-635.

Highlights

- Morpho-bathymetric description of a thin-skinned Fold-and-Thrust Belt.
- Evidence of strike-slip folding revealed by bathymetric, slope and 2-D seismic data.
- The folding is related to the present-day South American-Scotia plate boundary.

Esteban, Federico: Conceptualization, Methodology, Software, Writing- Original Draft.

Ormazabal, Juan Pablo: Visualization, Writing - Review & Editing.

Palma, Fermín: Visualization, Resources.

Cayo, Eric Lubin: Data curation, Resources.

Lodolo, Emanuele: Writing- Reviewing and Editing.

Tassone, Alejandro: Writing- Reviewing and Editing, Supervision, Funding acquisition, Project administration.

Declaration of interests

☒ The authors declare that they have no known competing financial interests or personal relationships that could have appeared to influence the work reported in this paper.

☐ The authors declare the following financial interests/personal relationships which may be considered as potential competing interests:

--